博 士 学 位 論 文
Doctoral Thesis

論文題目

Thesis Title

Research on Omnidirectional Series-fed Base Station Antenna for Sub-6 Band

（無指向性直列給電 Sub-6 帯基地局アンテナに関する研究）

東 北 大 学 大 学 院 工 学 研 究 科

Graduate School of Engineering,

TOHOKU UNIVERSITY

専攻/Department： Communications Engineering

学籍番号/ ID No： B9TD2302

氏 名 /Name： WU SIRAO（ウー スーラオ）

Research on Omnidirectional Series-fed Base Station Antenna for Sub-6 Band

(無指向性直列給電Sub-6帯基地局アンテナに関する研究)

by

Wu Sirao

A Dissertation
for Doctor of Philosophy (Engineering)

Submitted to
Department of Communications Engineering
Graduate School of Engineering
Tohoku University

July, 2023

Supervised by Prof. Chen, Qiang （陳　強）

Abstract

With the development of mobile communication, the innovation of communication methods has more demand for base station antenna. The new generation of mobile communication needs more base stations, more frequency band antennas to achieve better area coverage, as well as the diversity of frequency band and polarization. Small size, low cost, broadband and polarization diversity are the requirements for the new generation of mobile communication antennas. As a supplement, Sub-6 refers to the band below 6 GHz, which has less attenuation than millimeter wave and can cover a wide area. It is usually implemented with omnidirectional antennas. The series-fed array antenna can reduce the number of feed ports very effectively, which reduces the antenna design complexity while effectively reducing the size and cost of the antenna, making it ideal for application in small base stations.

In order to improve the bandwidth of the series-fed antenna, the technique of series-fed antennas discussed in this dissertation is introduced at first. Although the series-fed antenna has a simple structure and low cost, the problem of narrow band is to be solved. Two design methods for broadband antennas are proposed. First, a non-uniform series-fed antenna array is designed using the principle of multiple resonant antennas. Compared with the traditional uniform series-fed antenna, the gain bandwidth is improved very obviously. Applying it to the omnidirectional series-

fed array, broadband characteristics can be achieved. Second, a transposed excited series-fed dipole array is proposed inspired by the self-complementary antenna, and its impedance and gain bandwidth exhibit stability over a wide frequency band, reflecting very good broadband characteristics. These two methods provide ideas and methods for the bandwidth spreading of series-fed antennas.

Moreover, a novel feeding method for omnidirectional series-fed broadband dipole array antennas is proposed. Inspired by the feeding method of turnstile antenna, the omnidirectional radiation of the series-fed antenna is achieved by designing the arrangement position of the dipole unit and finally feeding it with one port. The array antenna is processed with a 1mm copper wire and fed with a coaxial structure in the center. It can be confirmed experimentally that the impedance bandwidth and 1 dB gain bandwidth are 26.9% and 22%, respectively. This study provides a good idea for the implementation of a series-fed broadband omnidirectional antenna.

Besides, the omnidirectional circularly polarized series-fed array antenna is discussed. Taking a high-gain omnidirectional series-fed circularly polarized antenna structure as an example, according to the defects of its structure itself (poor omnidirectional characteristics of radiation from phi component and differences in radiation from orthogonal components), two improvement proposals are made for better circular polarization characteristics. One, by rotating the open-end direction of the loop unit, the roundness of the antenna is improved. Second, by adding loop unit at the center of the array, the radiation of loop is enhanced to improve the circular polarization characteristics, which is expressed as the improvement of circular polarization gain. This proposal, which has a significant effect on the uniform radiation and circular polarization characteristic enhancement of circularly polarized series-fed base station antenna, is a research result that is highly evaluated in practical terms.

Contents

List of Figures

List of Tables

Chapter 1

Introduction

1.1 Background

Over several generations, mobile communication systems have evolved from a communications infrastructure to a living infrastructure. People's requirements for terminals are not limited to making calls and sending messages. The interconnection of people, machines and industry is reflected in the new generation of mobile communications. The fifth-generation mobile communication system (5G), which is being introduced in many countries, is expected to evolve into a social infrastructure that goes beyond the infrastructure of daily life, and the next generation, Beyond 5G (so-called 6G), is expected to integrate cyber space with the real world and play a central role as the backbone of Society 5.0 [1].

1.1.1 Features of 5G and Requirements for Base Station Antennas

Beyond 5G, which is aimed for, requires further advancement of the distinctive features of 5G and the inclusion of four new functionalities. Further advancement

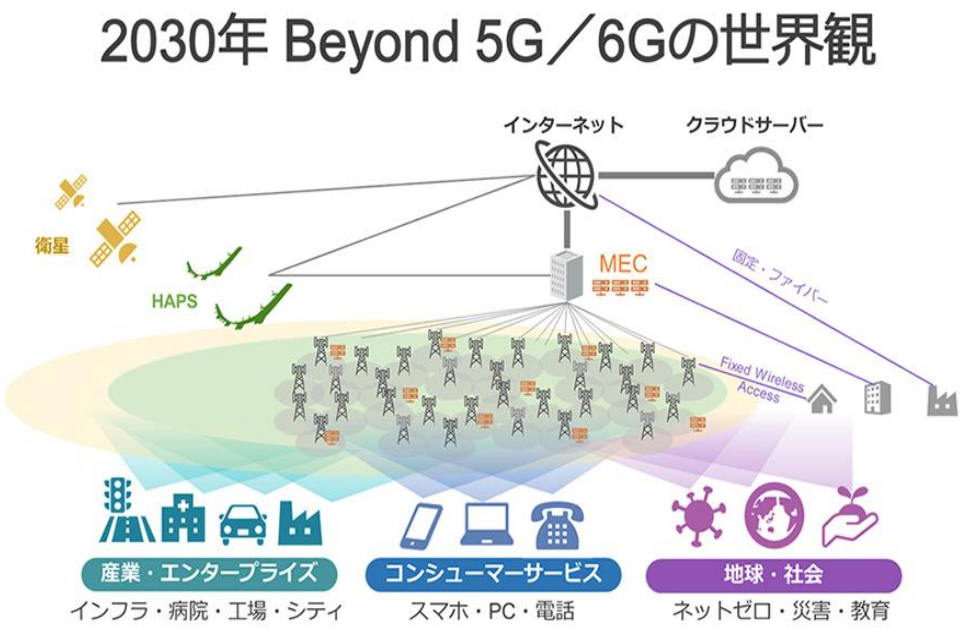

Figure 1.1: Beyond 5G Worldview [7].

of the distinctive features of 5G: the distinctive features of 5G should be further advanced to achieve functions such as "ultra-high speed and large capacity," "ultra-low latency," and "ultra-massive simultaneous connections," enabling the instant and accurate processing of massive data from any location. The features of 5G are shown as following:

1. Autonomy: Leveraging AI technologies, devices should autonomously collaborate without human intervention (zero-touch), establishing an optimal network instantly based on user needs without being conscious of wired or wireless connections.

2. Scalability: Terminals and base stations should seamlessly connect to different communication systems such as satellites and High Altitude Platform Stations (HAPS). Various devices, including terminals and windows, should function

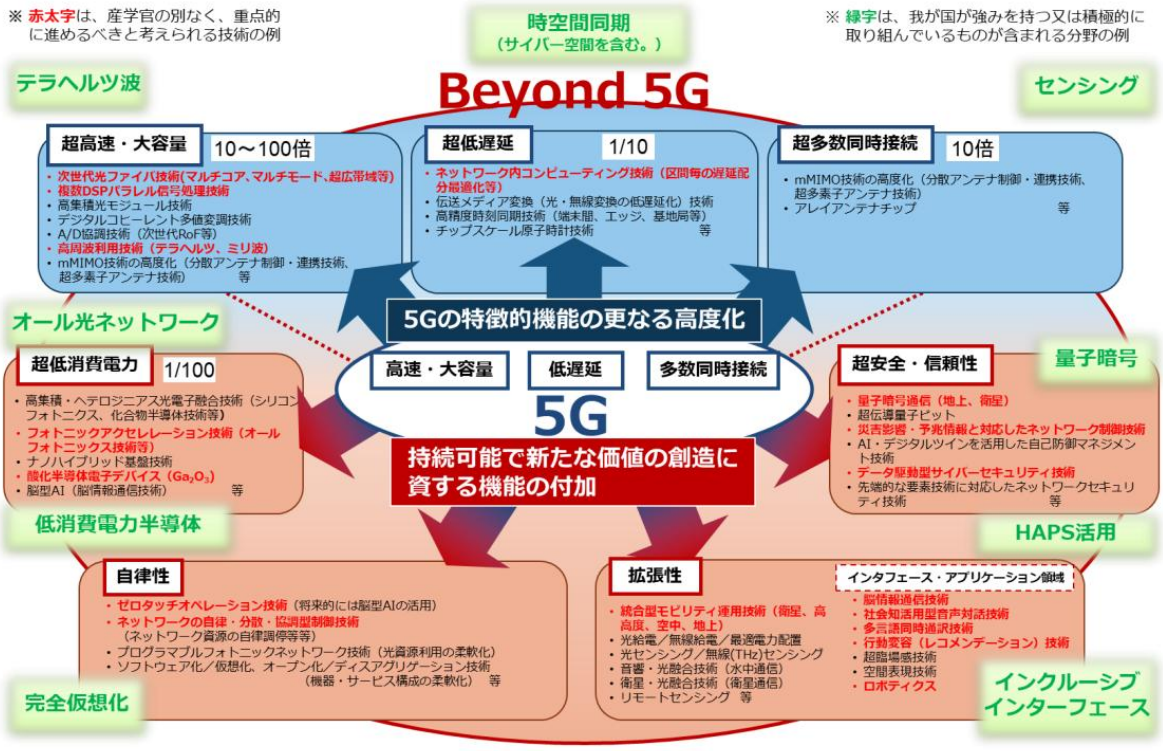

Figure 1.2: The features of 5G [1].

as base stations (ubiquitous base stations), enabling communication in every location, including land, sea, and space, while interconnecting with each other.

3. Ultra-security and reliability: Security and privacy should be consistently maintained without users having to be conscious of it. Services should remain uninterrupted even during disasters or failures, with instant recovery capabilities.

4. Ultra-low power consumption: Without the development of low power consumption technologies, it is estimated that the power consumption related to IT in 2030 will be 36 times that of 2016 (1.5 times the current total power consumption). To accommodate such a significant increase in power consumption, it is

necessary to consider reducing power consumption to approximately 1/100 of the current level.

In order to achieve "autonomy", more base stations or terminals will be put into use to provide more stable network and coverage, and to ensure the communication and normal use between devices. At the same time, more types of antennas for different applications and environments can better achieve "scalability". In order to achieve the communication "reliability", more stable antenna system needs to be implemented to ensure the communication stability in special environment, such as disaster [4]. At the same time, "Ultra-low power consumption", also on the power consumption of the base station put forward more demanding requirements. Under the demand of increasing the number and types of base stations, increasing the coverage area, and reducing the consumption of power, high gain, broadband, and the sharing of multiple polarization antennas are the requirements for the new generation of mobile communication antennas. Meanwhile, small size and low cost antennas will be the trend of development in the future when base stations are ubiquitous.

1.1.2 Expansion of Frequency Band

Frequency bands for 5G have also been updated to mmWave and sub-6 bands which can be seen in Fig. 1.3. Millimeter wave is mainly used in MIMO [5], the key technology of 5G, implemented with directional antennas. The Sub-6 band is usually used for communication with omnidirectional antennas.

Millimeter-wave refers to the frequency range of 30 GHz to 300 GHz. However, since the 28 GHz band used in Japan's 5G is in close proximity to the mmWave range, it is also referred to as mmWave for ease of use. Being in a higher frequency range than Sub-6, mmWave allows for wide bandwidth allocation, enabling high-speed

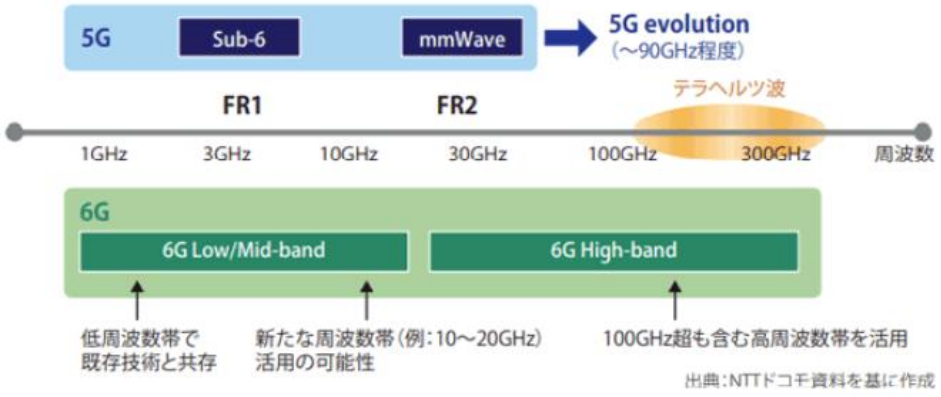

Figure 1.3: Developing frequency bands for 5G [3].

communication and supporting a large number of simultaneous connections. On the other hand, mmWave signals experience significant attenuation (weakening of the signal), resulting in a narrower coverage area. They also exhibit strong directional propagation, making them more susceptible to obstacles. Therefore, without some form of mitigation, mmWave technology may not cover a large area effectively. It is expected to be selectively used in congested areas or specific applications where its advantages can be utilized.

Sub-6 refers to the frequency range below 6 GHz. In Japan's 5G, the 3.7 GHz band and the 4.5 GHz band are used within this Sub-6 range. Compared to mmWave, Sub-6 experiences less signal attenuation, allowing the signals to reach wider areas, and they have the ability to propagate around obstacles.

Although millimeter wave can achieve ultra-high speed communication, but he is very sensitive to obstacles and can not achieve large coverage, and these disadvantages are exactly the advantage of Sub-6 band. In addition, millimeter wave base stations are more expensive, while Sub-6 base stations are relatively low-cost and can be integrated

into 4G base stations to achieve omnidirectional coverage. Although the shutdown technology for 5G is millimeter-wave MIMO, there is no substitute for a Sub-6 band base station as an aid.

In addition, the sparsely populated or small base station application scenarios need a wider coverage, simple system, low cost, and easy to build and maintain antennas. As an example, the Centralized Radio Access Network (C-RAN) deployment method used in beyond 5G communications, in which a central unit (CU) controls multiple distributed units (DU), helps achieve stable, high-quality, high-capacity communications regardless of location. By increasing the number of base stations per area and reducing the service area of one base station, C-RAN creates a communication-friendly environment even in crowded areas. Omnidirectional antennas are easy to implement in this case, with sufficient coverage and low cost compared to beamforming in the Sub-6 band [7].

1.2 Challenges of Base Station Antennas in Next-generation Mobile Communications

The development and implementation of 5G/B5G technology present several challenges that need to be addressed.

1. High gain VS size and cost

   B5G base station antennas need to accommodate a larger number of antenna elements. However, increasing the number of antenna elements can lead to larger antenna sizes and challenges in terms of physical size, weight, and form factor. Finding compact and aesthetically acceptable solutions for antenna deployment in various locations is a challenge. Fig. 1.4 show a variety of antenna arrays on

Tokyo Tower to meet different needs. The configuration of multiple antennas on the same base station is also a demand for future base station development.

Figure 1.4: Different kinds of antennas on Tokyo Tower [13].

In the pursuit of achieving high gain in antenna systems, the conventional approach often involves the establishment of large arrays. Large arrays bring problems such as complex feeding networks, mutual coupling, large size and expensive. Therefore, it is important to achieve small size while maintaining high gain. Series-fed antennas can be a good solution to the large size and high cost problems caused by complex feed networks.

Small base stations with high gain levels offer more possibilities to gather more antenna arrays on the same base station.

2. Bandwidth enhancement

   Broadband antennas can meet the requirements of different operators and different communication standards, support reliable communication, provide system possibilities for large file transmission, and enable infrastructure sharing.

   With the application of Sub-6 band, broadband antenna is still an important subject of antenna research. The trade off between bandwidth and gain, wide band radiation pattern and impedance matching, mutual coupling, size and cost are all challenges faced by wide band antennas.

3. Multiple polarization

   Linearly polarized antennas is commonly used now. Because linearly polarized antennas are simple in structure and easy to implement. It have developed from single polarization in 1983 to dual-polarized antennas. At present, positive and negative 45-degree polarized antennas are very wildly used base station antennas.

   B5G requires eliminating out-of-area coverage in residential areas and making all of the earth an area [7]. The problem can be solved by providing non-terrestrial network solutions that utilize low earth orbit and geostationary orbit satellites. With the demand of satellite communications, circularly polarized antennas is also necessary, it is harder to generate circularly polarized field comparing to linearly polarized antenna. If the circularly polarized antenna is used as transmit antenna, the multi-path effects can be avoided and provide stable signal transmission.

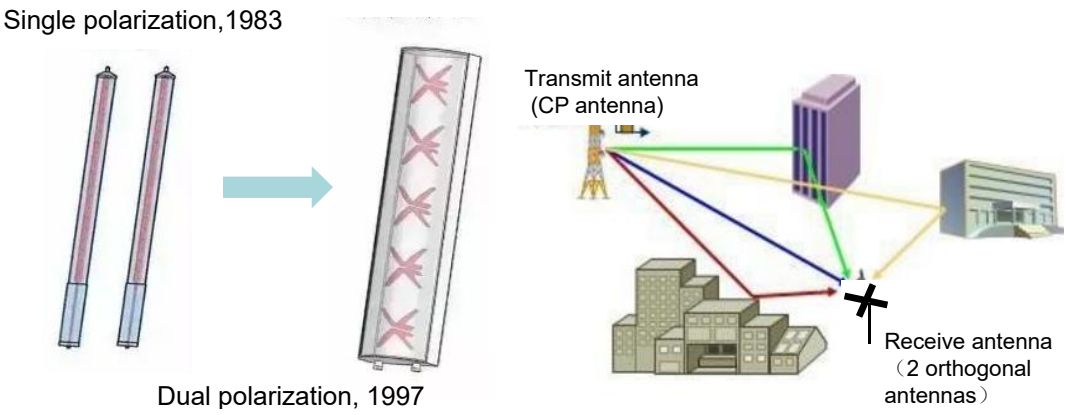

(a) Development of linearly polarized base stations [8].

(b) Transmission system of circularly polarized antenna [9].

Figure 1.5: Base station requirements for polarization.

1.3 Implementation of Omnidirectional Base Station

There are two main implementation methods of the omnidirectional base station antenna. One is to use an omnidirectional antenna as a unit, such as a super turnstile unit, it is for television broadcasting. Another example is helical antenna array for satellite communications. The other implementation of omnidirectional base station is muti-side synthesis of directional antenna. Twin loop antenna is one of the examples which is wildly used in Japan for radio broadcasting [13, 14].

(a) Super turnstile antenna for television broadcasting in Germany [10].

(b) Helical antenna array for satellite tracking-acquisition in France [11].

(c) Twin loop antenna array for radio broadcasting in Japan [12].

Figure 1.6: Implementation of omnidirectional base station.

1.3.1 Super Turnstile Antenna

Turnstile antenna is an example which use omnidirectional antenna as unit for base station.

The turnstile antenna was invented in 1935 by George H. Brown at RCA Corporation in the United States. The antenna used for broadcasting at VHF and UHF frequencies is known as a batwing or super turnstile antenna because of its unusual design, which resembles a bat wing or bow tie. Due to its omnidirectional properties, batwing antennas are utilized in stacked arrays for television broadcasts [15].

A specialized form of crossed dipole antenna, or a variation of the turnstile antenna, called batwing antennas. Like the configuration in Fig. 1.6, around a single mast, two pairs of identical vertical batwing-shaped pieces are attached at right angles. A dipole is supplied by element "wings" on opposing sides. The two dipoles are supplied 90 degrees out of phase in order to produce an omnidirectional pattern. In the horizontal plane, the antenna emits radiation that is horizontally polarized. A bay is a collection of four items on a single level. Despite having four tiny lobes (maxima) in the directions of the four elements, the radiation pattern is almost omnidirectional. The multi-element antenna system for television transmission that emits waves that are horizontally polarized. By focusing radiation in the horizontal direction at the expense of radiation in the vertical direction, a greater gain is achieved. The antenna's gain rises with the number of sections or layers utilized, although there is a limitation set by practical factors [16–19].

In the actual assembly, we mentioned that the batwing unit needs to be supported with mast, so the tower supporting the antenna must be thin compared to the wavelength. Therefore, for thicker towers, other types of antennas must be adopted. This inspired us to use turnstile antenna as omnidirectional base station antenna, which is

more suitable for narrow environment and meets our requirement of miniaturization for new generation mobile communication base station, because it does not need reflector. However, when turnstile antenna is fed in practical, it needs a lot of cables or power dividers to realize the excitation of the array, which means the overall size of the antenna will be bigger again. If this problem can be solved, this antenna will be a good choice for miniaturized base station antenna.

1.3.2 Muti-side Synthesis Array Antenna

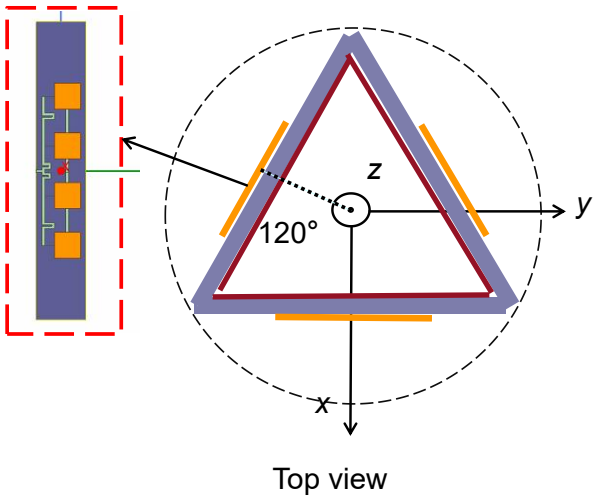

Figure 1.7: Dual-polarized omnidirectional antenna for Sub-6 base station [20].

Fig. 1.7 shows an example of muti-side antenna array which composed of three sides. It realizes dual polarization. The antenna consists of three planar arrays like a trihedron, and the angle between each planar is 120 deg. The array is fed with comb-shape and string-shape series feeding methods to achieve horizontal polarization and vertical polarization respectively which means both polarization shares the patches. Since the structure of each side is consistent, the design is simple. However,

the addition of the ground will make the size of the antenna limited, and the large size will be its disadvantage compared with the implementation that directly using omnidirectional antenna as a unit. So for compact application, the omnidirectional antenna unit is better.

1.4 Organization of this Dissertation

This dissertation is structured into five chapters, providing a comprehensive investigation into various aspects of omnidirectional series-fed base station antenna for Sub-6.

Chapter 1 serves as the introduction, talking about the background and the challenges associated with traditional array configurations. It establishes the motivation and objectives of the study.

Chapter 2 delves into the concept of broadband series-fed antenna arrays, two methods for broadband are proposed. One is non-uniform array, the other is transposed excited array. It is verified that the bandwidth of series-fed dipole array could be effectively broadened by both methods.

Chapter 3 presents a novel feeding method for broadband series-fed antennas to achieve omnidirectional radiation patterns. The 90 deg phase difference is achieved by putting the crossed dipoles at a distance of a quarter wavelength. And the transposed excitation is also applied in the proposed antenna.

Chapter 4 shifts the focus to circularly polarized series-fed antenna arrays. Methods are proposed for omnidirectional circularly polarized (OCP) antennas of omnidirectional property and high gain. By adjusting the open-end orientations of the loops, the non-omnidirectional pattern caused by the non-uniform currents of half-wavelength loops has been significantly improved. And a center loop loaded ten-stage OCP an-

tenna array effectively enhanced the radiation of magnetic radiator for better circularly polarized property.

Chapter 5, encompasses the conclusions. It summarizes the contributions, and implications of the study. Additionally, the chapter outlines potential avenues for future research and highlights the significance of the research outcomes in advancing the field of antenna engineering.

Chapter 2

Broadband Series-fed Base Station Antenna Array

In this chapter, we briefly introduce the series-fed antenna technology. We discusse the bandwidth broadening issues of the series-fed antenna. Two main methods are presented: one is the non-uniform series-fed dipole array, and the other is the transposed excited dipole array. Through simulations, both methods have extended the gain bandwidth compared to the regular fed dipole array.

2.1 Feeding Methods of Antenna Array

The primary purpose of the array's feeding network is to control the amplitude and phase of each individual element, enabling the formation of the desired radiation pattern or optimization of specific antenna performance metrics. The most commonly employed feeding network configurations are series feeding and parallel feeding, with certain larger arrays incorporating a hybrid combination of both series and parallel

feedings.

2.1.1 Parallel Feeding Technology

Parallel feeding is usually done with several power dividers that distribute the input power to individual elements. The parallel feeding form shown in the Fig. 2.1 is the most common form of multi-stage two-way power distribution. When all elements in the parallel feed array are the same, then the amplitude can be controlled by changing the power divider, and the phase can be controlled by using the change in length of each feed line or the phase shifter. The equal length feed line can realize uniform distribution and achieve the maximum gain. For phased array antenna, the electronically controlled phase shifter can achieve the phase distribution required for beam scanning.

Compared to series feeding, parallel feeding has some unique advantages. The required excitation amplitude and phase of each element can be realized by designing the feeding network, and the design method is simple and straightforward. In a homogeneous array, a broadside array is formed, and the beam direction is independent of frequency, so the bandwidth mainly depends on the bandwidth of elements, and it is relatively easy to achieve a wide bandwidth. But the parallel feed also has its significant disadvantage, when the number of array elements is large, the feeding network is graded more, the total length of the feed line becomes longer, which makes the antenna array bulky. The transmission loss also increases, so that the array feeding efficiency is reduced, and the whole feeding network becomes complicated. This feeding method does not meet the requirements for a new generation of mobile communication base station antenna miniaturization.

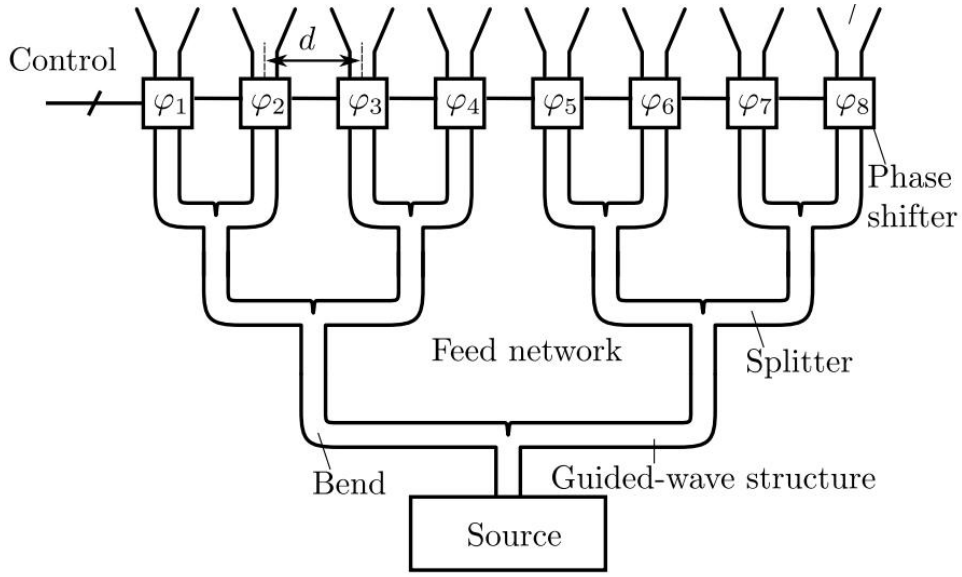

Figure 2.1: Parallel feeding by using multi-stage two-way power dividers [21].

2.1.2 Series Feeding Technology

The series feeding is to use the transmission line to connect all the antenna elements in series. Series feeding are usually available in two forms. The first is a feed line that directly connects the radiating elements, as shown in Fig. 2.2(a), and is shaped like a barbecue skewer. The other, as shown in Fig. 2.2(b), has a main feed line that distributes the excitation current to each element and is shaped like a comb. The phase distribution of the current can be achieved by adjusting the spacing between the elements, and the current amplitude distribution of the elements can be changed by adjusting the size of the elements or the width of the feed line. Resonant series feeding has narrow-band operating characteristics because it operates in a resonant state. The change in frequency leads to a change in phase and a change in beam inclination. However, because this type of feeding does not need to add terminal matching loads

and is simple and compact, the transmission line has low stray radiation, low losses and high feeding efficiency. Because of these advantages, this feeding method is widely used and is suitable for 5G/B5G system.

(a) Barbecue-shape series feeding array [22].

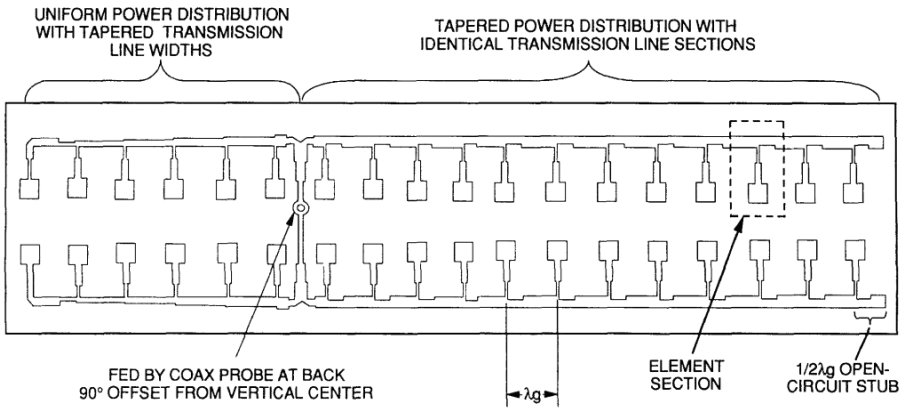

(b) Comb-shape series feeding array [23].

Figure 2.2: Different kinds of series-fed arrays.

2.2 Previous Studies of Series-fed Dipole Arrays

There are many studies on broadband series-fed dipole arrays, but most of them are end-fire [24–28]. As shown in Fig. 2.3, a coplanar strip (CPS) line-fed series dipole array antenna is proposed [28]. The CPS line is used to link printed dipoles of the same size, and an integrated balun is used to ensure impedance matching. The antenna radiates

horizontally polarized wave with broadband. However, in omnidirectional radiation applications, broadside antennas are more desirable.

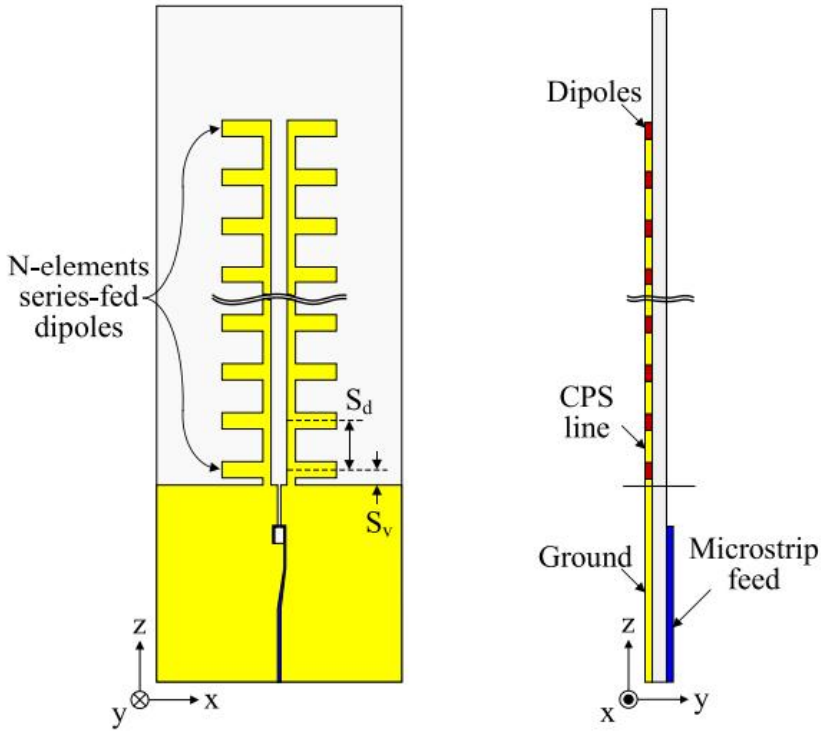

Figure 2.3: End-fire CPS line-fed series dipole array antenna [28].

In Ref. [29], a broadside omnidirectional series-fed dipole array antenna is proposed which is shown in Fig. 2.4. With a relative bandwidth of 4.5%, a maximum gain of 10.3 dBi is achieved. The proposed antenna is vertically polarized. There are several drawbacks of this antenna in compact base station application. Firstly, the bandwidth is narrower. Secondly, the full length is 6.23 wavelength and the size is larger. Thirdly, the microstrip grounded coplanar waveguide (MS-GCPW) feed needs to be designed, and the feed design is relatively complicated.

This chapter mainly study the series-fed dipole array of broadside.

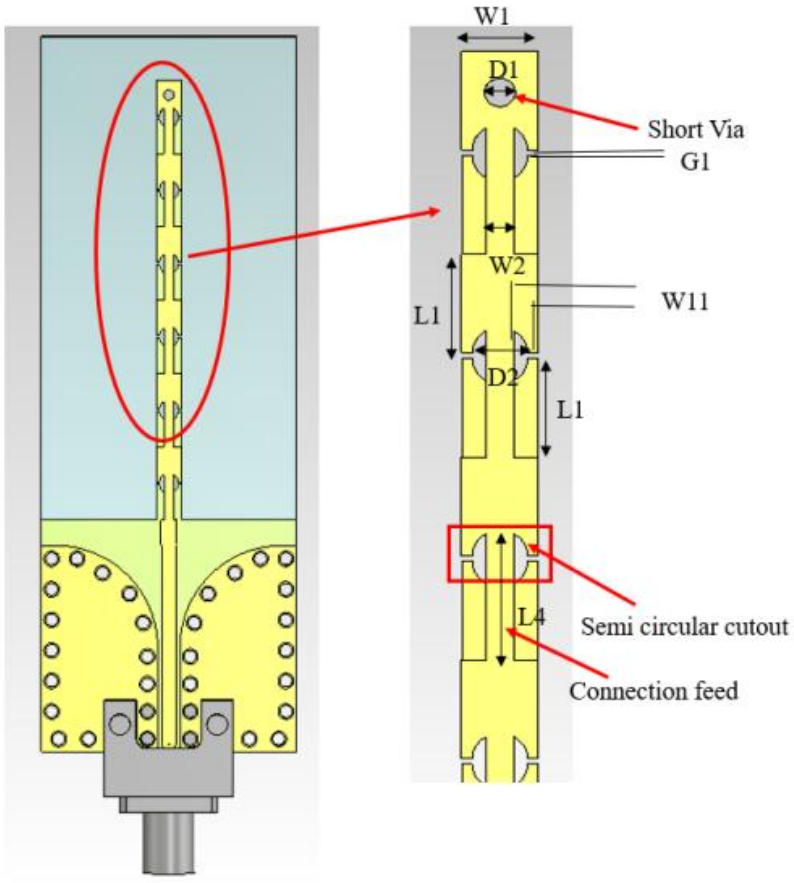

Figure 2.4: Broadside series-fed omnidirectional mm-wave dipole array [29].

2.3 Broadband Series-fed Base Station Antenna Array

In the pursuit of achieving higher gain, certain researchers have employed a selection of specially constructed horizontally polarized (HP) antennas to establish an antenna array. Within the realm of mobile communications, an intriguing study [30] introduced a broadband HP omnidirectional planar antenna featuring arc dipoles. This antenna design exhibits a remarkable peak gain of 8 dBi. However, a notable

drawback of this antenna configuration is its substantial size, exceeding 6λ, and its reliance on a significant number of feeding wires, resulting in a bulkier and more intricate system. Additionally, researchers have explored the implementation of traveling wave antennas to attain high gain omnidirectional HP radiation [31]. However, an inherent characteristic of these antennas is the variability of their beam patterns across different frequencies. This variability poses a challenge in achieving consistent and reliable performance. Furthermore, a slender Fabry-Perot antenna has been proposed as an alternative solution for achieving high gain in [32]. This antenna design successfully reached a realized gain of 8.52 dBi within the frequency range of 2.41 to 2.5 GHz, accompanied by an impressive 10 dB impedance bandwidth. The prototype of this antenna adheres to a compact size of 2.95λ, showcasing an intended focus on miniaturization. Nevertheless, the most significant limitation of this antenna design lies in its restricted bandwidth, accounting for only approximately 3.75% of the operational frequency range. This constraint emerges as the most prominent flaw, potentially limiting its applicability in scenarios requiring broader frequency coverage.

We think that the turnstile antenna form is more suitable for miniaturized omnidirectional base station applications. Combined with series-fed technology, it can effectively reduce the number of ports. In this chapter, for the narrow band problem of series-fed antenna, two methods are proposed to widen the bandwidth under the structure of series-fed dipole array. The first one is to use non-uniform array, compared with uniform array, the gain bandwidth is significantly improved, and apply it to the omnidirectional antenna, and also confirm to the bandwidth spreading characteristic. The second one is transposed excited dipole array. By simulation, the bandwidth of the array antenna is effectively broadened compared to the conventional feeding case.

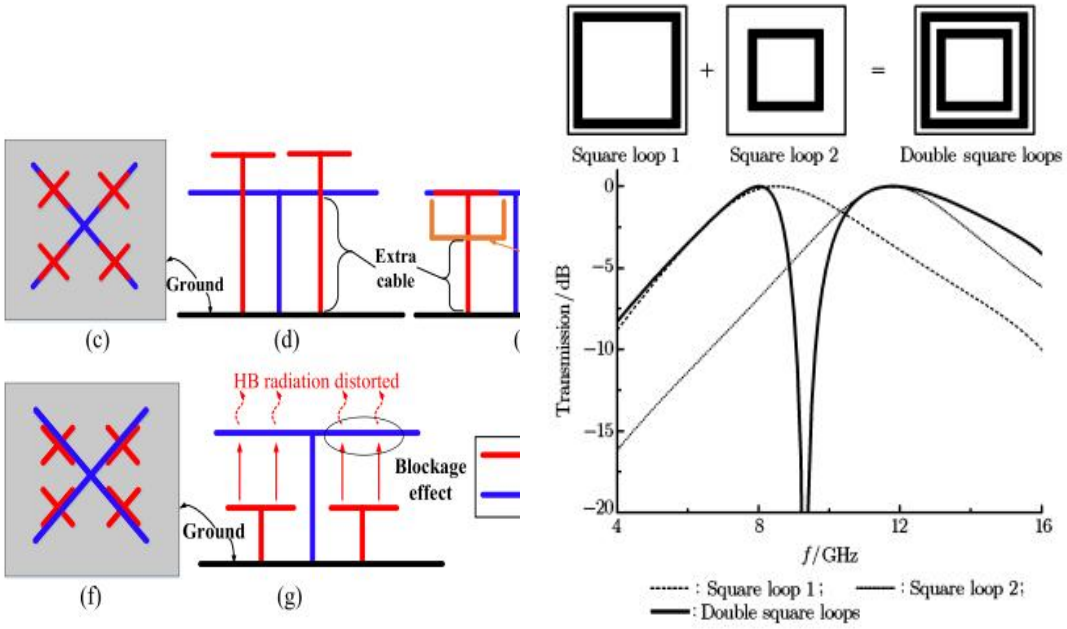

(a) Broadband electromagnetic-transparent antenna [33].

(b) Frequency selective surface(FSS) [34].

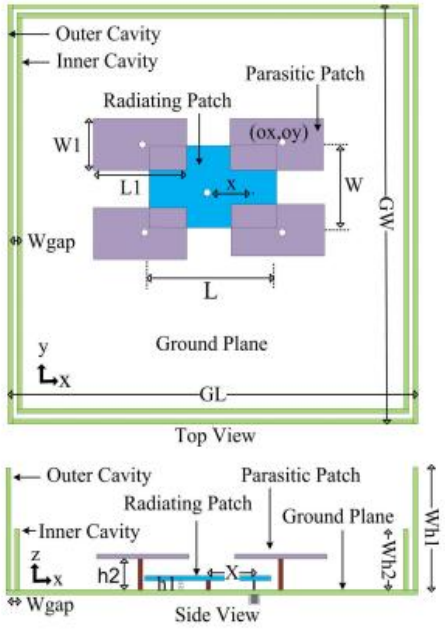

(c) Parasitic loaded antenna [35].

Figure 2.5: Applications of multiple resonances.

2.3.1 Non-uniform Series-fed Dipole Array

According to our cognition, based on the array antenna theory, when all the units are the same, the array will produce a very strong radiation at a certain frequency. However, when the units are not the same, this very strong radiation at the certain frequency will be disrupted and the radiation spread to other frequencies. Eventually, broadband will be achieved by sacrificing the gain.

Many researchers use multiple resonance to explain the phenomenon of using antenna size changes to generate broadband characteristics. Multiple resonance refers to different antenna elements for radiation at multiple frequencies, and each element contributes to the antenna's overall bandwidth. As shown in Fig. 2.5, multiple resonance is used in many designs. Fig. 2.5 is a geometry of broadband base station array [33]. Different sizes of cross dipoles correspond to different frequencies of radiation. The antennas Share the same aperture and the design is simple. The main drawback is the upper layer block and complex feeding network. Another application is frequency selective surface [34]. The pass band is determined by adjusting the size of elements. In addition, it is also used in parasitic loaded antennas. The bandwidth is broaden by introducing new resonance through parasitic elements [35].

We put forward a proposal to use dipole units of different lengths to break the strong radiation of dipole arrays of the same length at a certain frequency to achieve the effect of bandwidth. The geometry of the proposed antenna is shown in the right of Fig. 2.6. The construction of the antenna array involves a systematic arrangement of dipole elements, with their characteristics varying along the array. Each dipole element in the upper half is labeled as No. n starting from the center. The length of the No. n element is denoted as l_n, while the separation between element No. n and element No. n+1 is represented by d_n.To achieve the desired design, the length of

each dipole element undergoes a linear reduction from the first dipole element in the middle to the fifth dipole element at the end of the parallel strip line. Specifically, the length of each dipole element decreases by l_m with respect to its preceding element. Similarly, the distance between the dipole elements also experiences a decrease from each preceding dipole spacing. This reduction in spacing, denoted as d_m, is consistent with the decrease in dipole length.

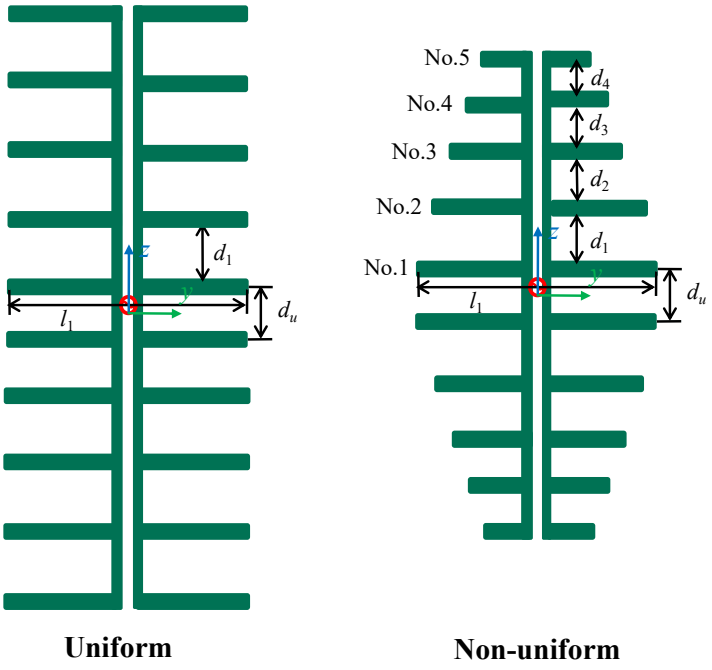

Figure 2.6: Structures of uniform and non-uniform series-fed dipole arrays.

For a uniform array configuration, each dipole element's length remains constant and equal to half a wavelength at the design frequency of 4 GHz (In Japan, 3.7-4.9 GHz from Sub-6 band has been applied). To ensure that the elements radiate in phase, the separation between the elements on the feeding line is maintained at one wavelength. Both the structures of uniform and non-uniform case is shown in Fig. 2.6.

In a case of non-uniform arrays, the No. 1 dipole element is positioned close to the center and has a length equal to half a wavelength. Subsequently, each successive dipole element is 1.875 mm shorter than its preceding element. The separation between the No. 1 and No. 2 dipole elements is precisely one wavelength, and the distance between each subsequent element is reduced by 3.75 mm. By carefully manipulating the lengths and separations of the dipole elements, the array configuration can be customized to achieve desired radiation characteristics and performance metrics.

The upper half geometry under the condition of different length changes l_m is shown in Fig. 2.7(a). It can be seen that the larger the l_m is, the smaller the dipole unit far away from the center is.

Furthermore, Fig. 2.7(b) depicting the maximum directivity in the horizontal plane is provided, showcasing the impact of different l_m values. Each l_m value is represented by a distinct color, indicating varying rates of change. It becomes evident that as l_m increases, the 3 dB bandwidth of gain expands. However, there is a notable trade-off: the maximum gain experiences a sharp decrease with the increasing l_m values.

Similarly, the geometry under the condition of different distance changes d_m is shown in Fig. 2.8(a). It can be seen that the larger the d_m is, the shorter distance of adjacent dipoles is.

Fig. 2.8(b) illustrates the maximum directivity in the horizontal plane as a function of varying d_m values. Each d_m value is represented by a unique color, denoting different rates of change. An observation can be made that as d_m increases, the maximum gain tends to shift towards higher frequencies. This indicates that the peak gain of the antenna occurs at higher frequency ranges when larger d_m values are employed. On the other hand, the bandwidth remains relatively constant across the different d_m values. This suggests that the frequency range over which the antenna maintains a desirable level of gain remains largely unaffected by changes in d_m.

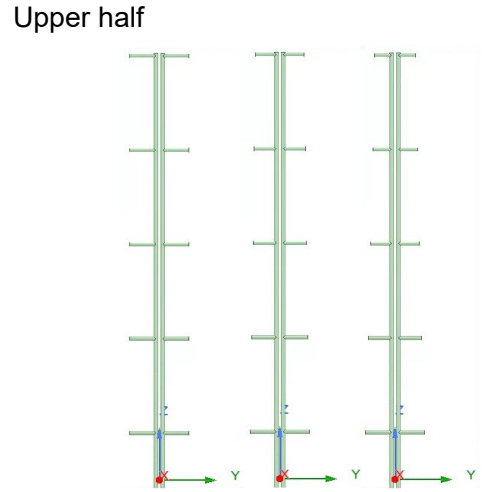

l_m (mm)	0	1.875	3.75
	uniform	non-uniform	
Band width	13%	15%	25%

(a) Geometry.

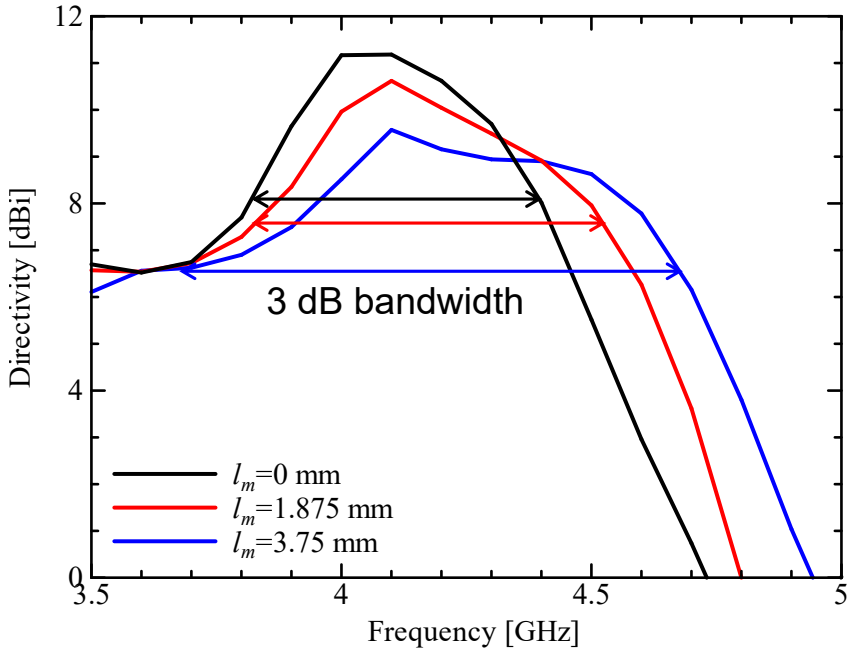

(b) Directivity.

Figure 2.7: The characteristics of the antenna vary with l_m.

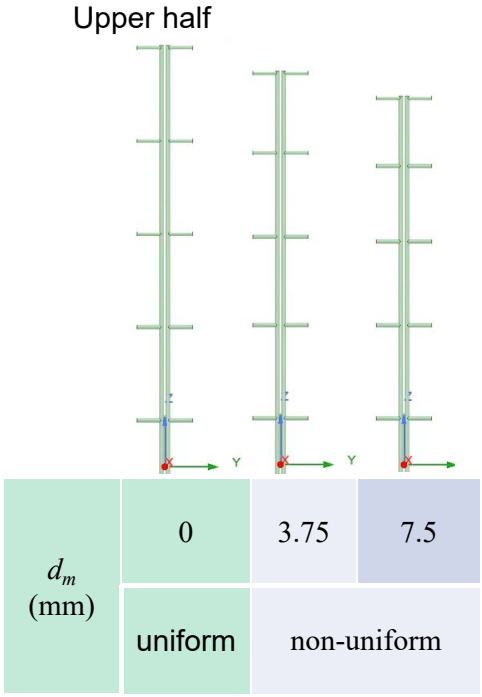

(a) Geometry.

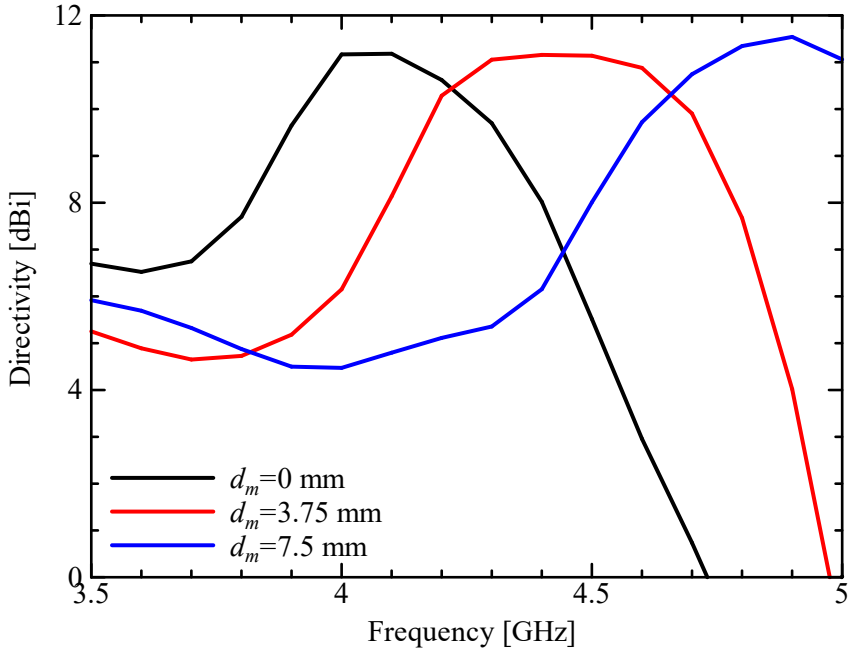

(b) Directivity.

Figure 2.8: The characteristics of the antenna vary with d_m.

Therefore, lm primarily affects the gain bandwidth and the maximum gain, dm primarily affects the frequency at which the antenna achieves its maximum gain, while the overall bandwidth remains stable. These findings highlight the significance parameter selection in determining the frequency characteristics and performance of the antenna.

The length of the dipole starts from half a wavelength of 4 GHz as the initial value. In order to maintain the same phase current on the dipole unit, the initial distance is one wavelength. Since our desired frequency is 4-5 GHz, considering both the gain level and bandwidth, by parameter study, the parameters are chosen as follows in Table 2.1. We compare the uniform structure with the non-uniform structure to verify the broadband characteristics.

Table 2.1: The parameters of non-uniform series-fed dipole array.

Prameters	Uniform (mm)	Non-uniform (mm)
l_1	37.5	37.5
d_1	75	75
d_u	50	50
d_m=d_n-d_{n+1}	0	3.75
l_m=l_n-l_{n+1}	0	1.875

Fig. 2.9 includes radiation patterns at different frequencies, with dashed lines representing uniform structures and solid lines representing non-uniform structures. Across both cases, it can be observed that the radiation patterns exhibit an 8-shape pattern at the presented frequencies. This indicates a certain level of directivity and specific radiation characteristics associated with the antenna design. Additionally, the maximum gain value demonstrates variation with changing frequencies.

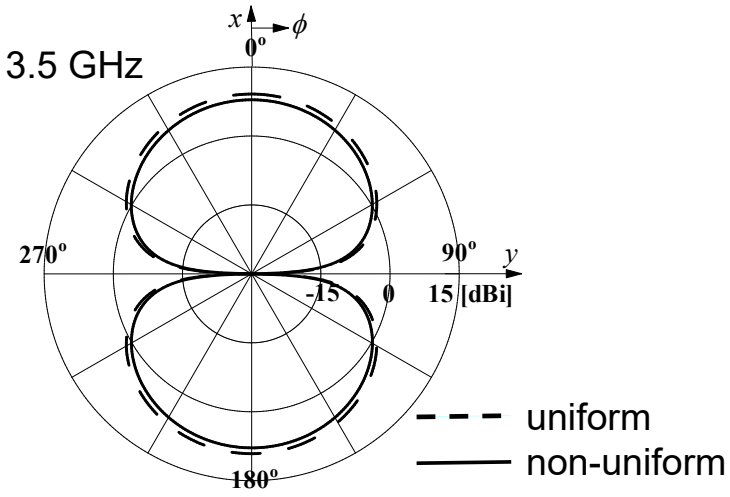

(a) 3.5 GHz

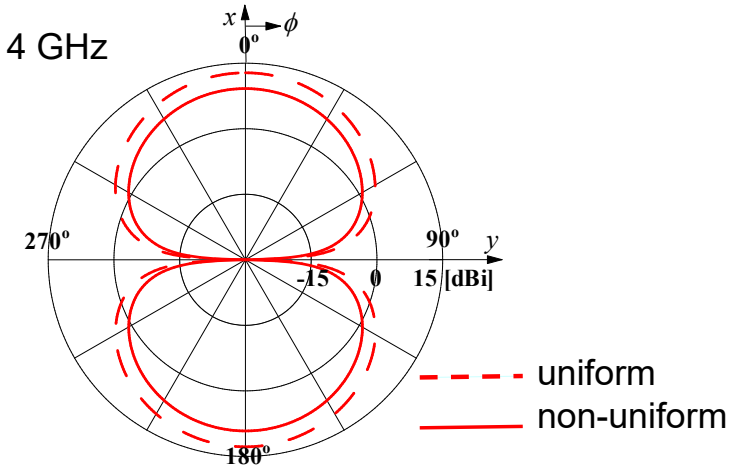

(b) 4 GHz

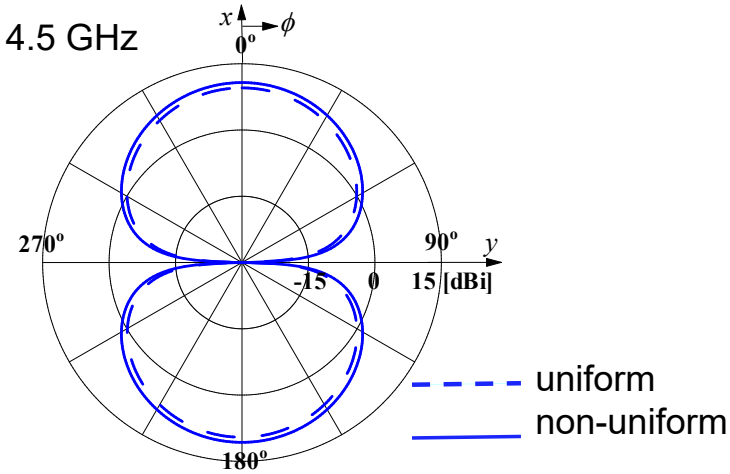

(c) 4.5 GHz

Figure 2.9: The radiation patterns at different frequencies.

Fig. 2.10 illustrates the relationship between directivity and frequency. Notably, the non-uniform series-fed dipole array exhibits a 3 dB gain bandwidth that spans from 3.5 to 5 GHz. This range of frequencies surpasses the corresponding bandwidth achieved by the uniform array configuration. In comparison to the uniform array, the non-uniform series-fed dipole array experiences a reduction in maximum gain of approximately 2 dB. This indicates that, while the non-uniform array offers a wider bandwidth, there is a trade-off in terms of the highest achievable gain.

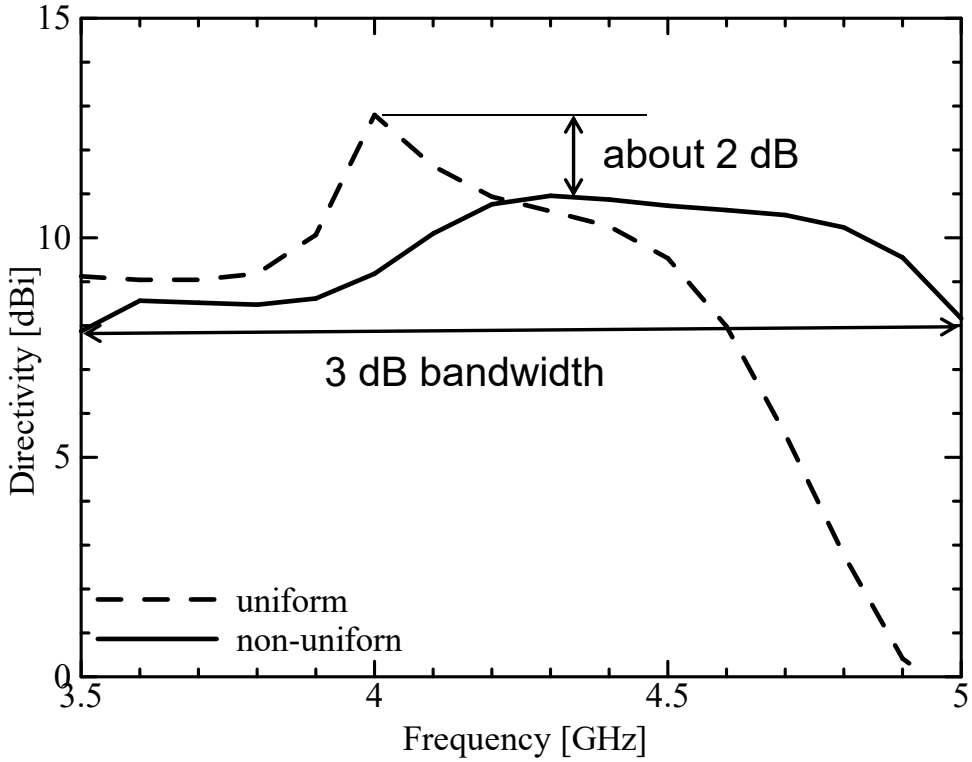

Figure 2.10: Maximum directivity in horizontal plane.

Next, we use the non-uniform series-fed array to achieve omnidirectional radiation patterns. Two identical planar non-uniform arrays are placed orthogonally and excited with 2 ports in a 90-degree phase difference. The geometry of omnidirectional non-

uniform array is shown in Fig. 2.11.

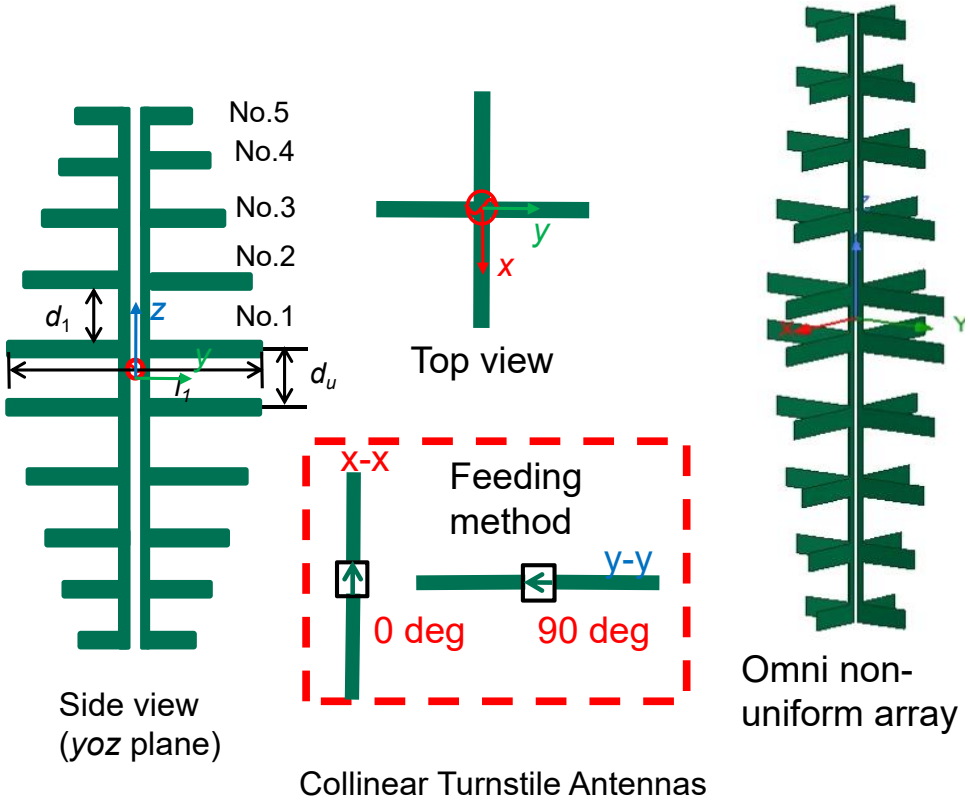

Figure 2.11: The geometry of omnidirectional non-uniform array.

Fig. 2.12 shows radiation patterns at different frequencies. At the presented frequency band, it can be observed that both the non-uniform and uniform arrays achieve omnidirectional radiation patterns. Furthermore, the maximum gain value demonstrates variation with changing frequencies.

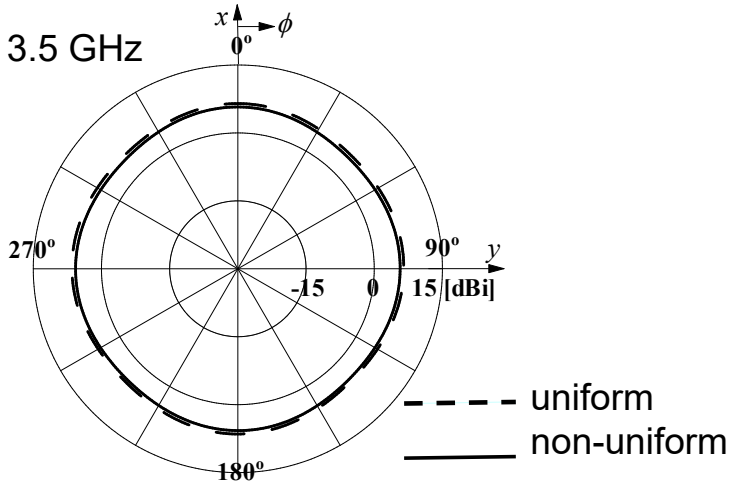

(a) 3.5 GHz

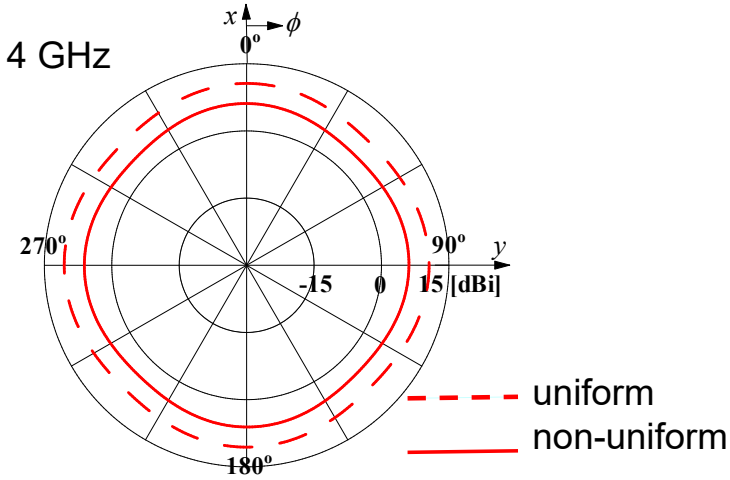

(b) 4 GHz

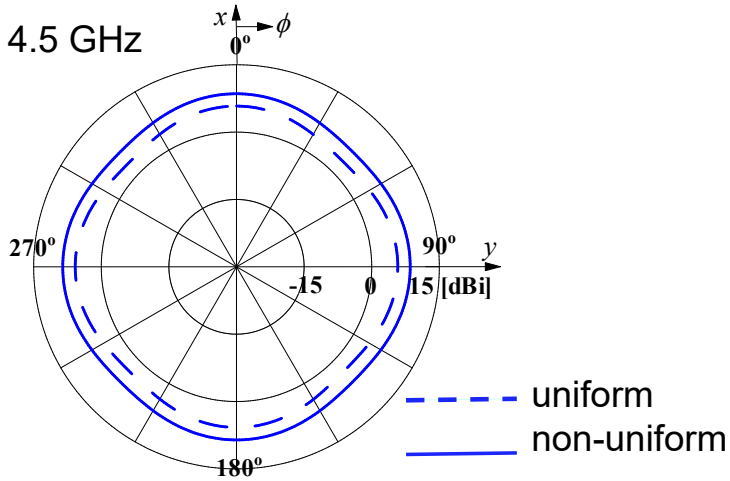

(c) 4.5 GHz

Figure 2.12: The omnidirectional radiation patterns at different frequencies.

The maximum directivity of omnidirectional antenna is shown in Fig. 2.13. The gain bandwidth of the non-uniform antenna array remains superior, surpassing that of the uniform antenna array by 20.7%. This indicates that the non-uniform array configuration exhibits a wider operational bandwidth compared to the uniform array.

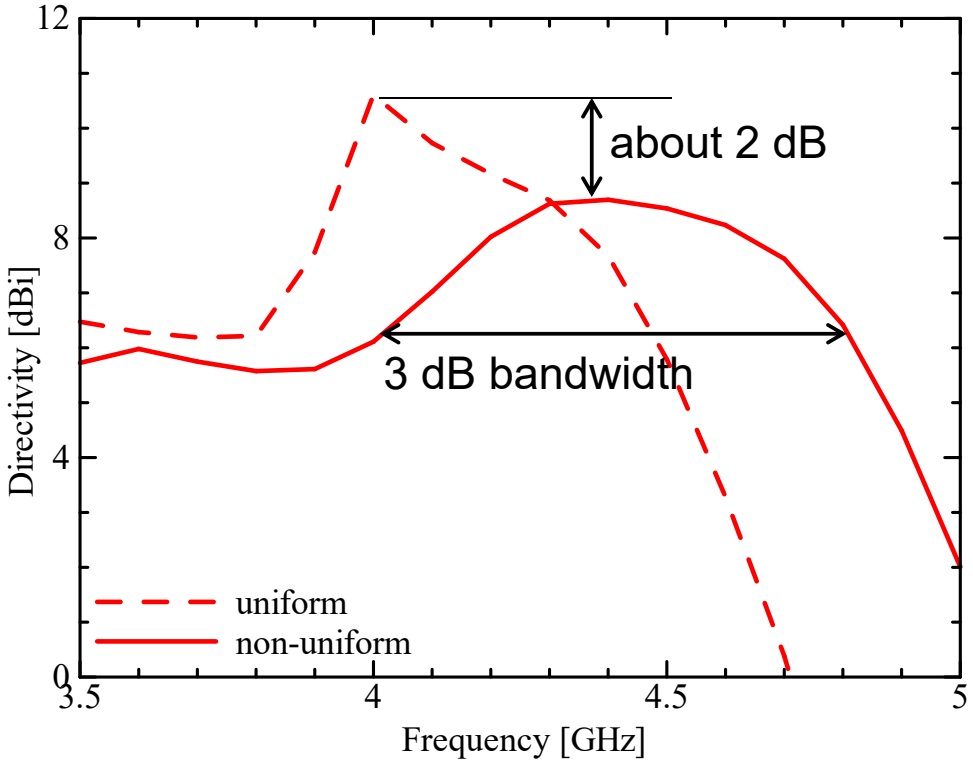

Figure 2.13: Maximum directivity of omnidirectional antenna in horizontal plane.

So far, the effectiveness of achieving wideband performance through the implementation of non-uniform arrays has been confirmed. The wider bandwidth offered by non-uniform arrays presents a notable advantage, enabling better compatibility with a range of frequencies and applications.

2.3.2 Transposed Excited Series-fed Dipole Array

The other broadband method is inspired by self-complementary antenna. The concept of self-complementary antenna was introduced by Prof. Mushiake in 1948. This method involves designing the complementary structure of the antenna to be exactly identical in shape to the original part. An important characteristic of this method is that the input impedance of the antenna remains constant which achieves a broadband response [36]. It should pay attention that “Log-Periodic Antenna” is a modified self-complementary antenna. Prof. Mushiake said the LPDA does not have broadband property unless it has transposed excitation [37].

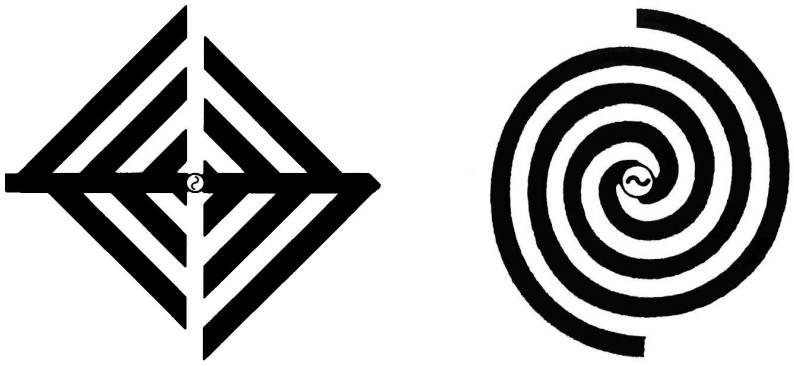

Figure 2.14: Typical self-complementary antennas [36].

We proposed a structure of modified transposed excitation for broadband series-fed dipole array shown in Fig. 2.15.

As depicted in Fig. 2.15, the proposed modified transposed excited series-fed dipole array is designed with a symmetrical configuration. The arms of the adjacent dipole are rotated 180 degrees on the main feeding line, forming a transposed excitation. This configuration results in a 180 degree phase difference between adjacent dipole units.

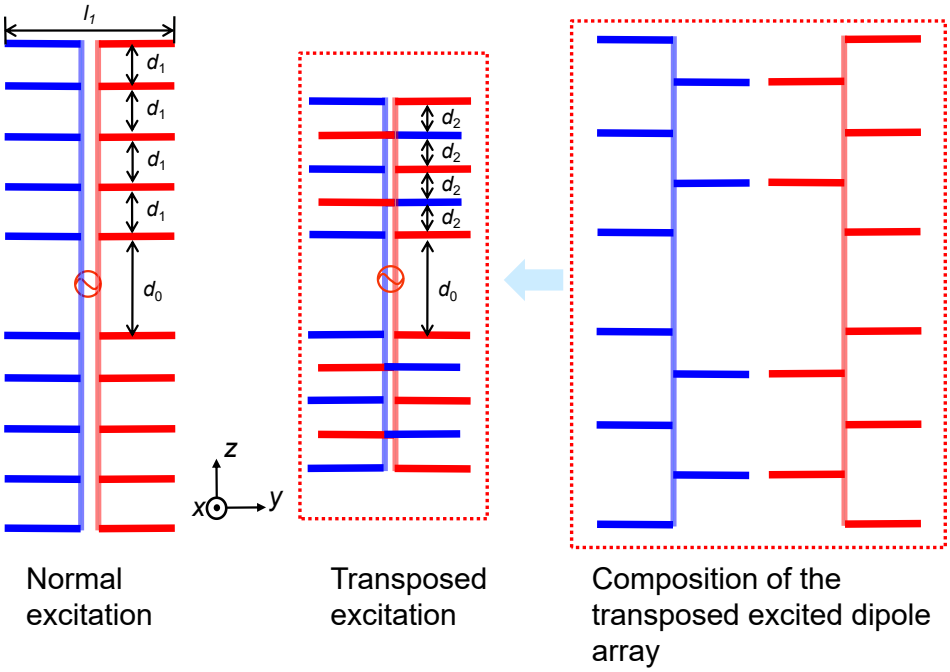

Figure 2.15: The geometry of modified transposed excited series-fed dipole array.

To achieve in-phase feeding of the dipole array, the spacing between adjacent units will be changed from one wavelength (normal excitation) to half wavelength. The parameters are shown in Table 2.2.

Table 2.2: The parameters of normal and transposed excited series-fed dipole arrays.

Prameters	Values (mm)
l_1	37.5
d_0	50
d_1	75
d_2	37.5

The proposed antenna is evaluated in terms of both impedance bandwidth and gain bandwidth. Impedance reflects the matching capability between the antenna and

the system. The smoother the impedance changes in the frequency band, the easier the matching between the antenna and the system will be. In addition, the broadband impedance matching can be obtained by designing a matching circuit. However, the gain bandwidth characterizes the stability of the antenna current distribution. The current distribution is determined on the antenna, which is directly related to radiation and is very important.

Fig. 2.16 shows the impedance of the dipole array in two scenarios: with and without transposed excitation. When normal excitation is used, both the real and imaginary parts of the impedance show a large tendency to fluctuate. This means that impedance matching is more difficult. In the case of the transposed excited dipole array, it can be observed that the impedance changes very smoothly across the frequency range. Specifically, the real part of the impedance remains almost constant within the 4-5 GHz frequency range. The smooth and consistent behavior of the impedance in the transposed excited dipole array leads to great broadband properties.

Fig. 2.17 presents the radiation pattern and directivity of the dipole arrays. Figure 2-17(a) depicts the radiation pattern in the horizontal plane specifically at 4 GHz. Both cases exhibit an 8-shape patterns, indicating similar radiation characteristics for both the normal excited array and the transposed excited array. Figure 2-17(b) illustrates the directivity in the horizontal plane. It is observed that the 3 dB gain bandwidth of the transposed excited array covers a wider frequency range, ranging from 3.5 to 4.9 GHz. This is a significant improvement compared to the normal excited array, demonstrating a much better ability to operate over a broader frequency range.

So far, the achievement of wideband performance through the implementation of the modified self-complementary structure has been confirmed. The use of the transposed excitation approach, along with the self-complementary structure, has proven effective in achieving wider bandwidth in both impedance and gain characteristics.

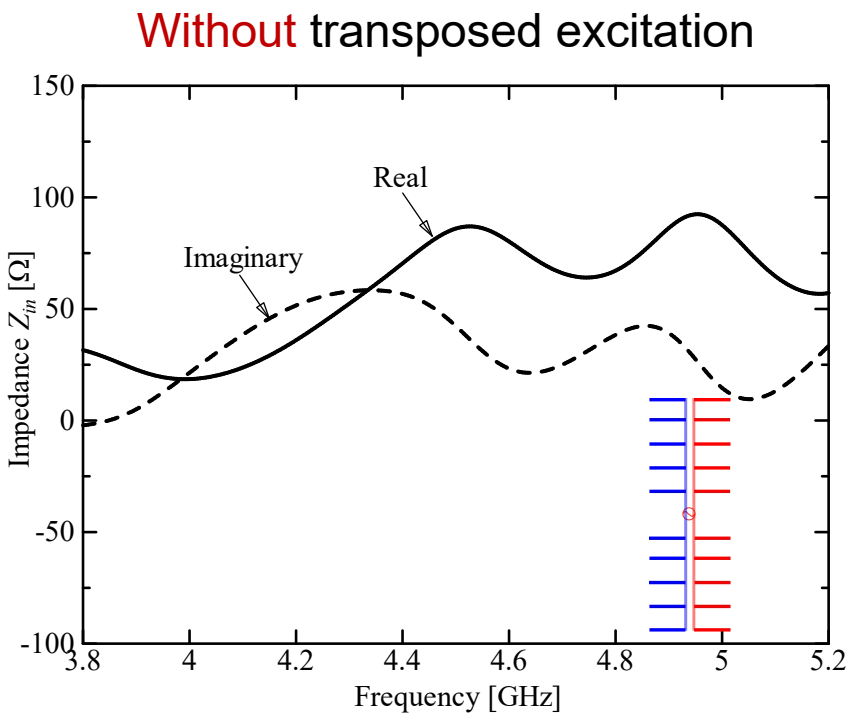

(a) Normal excitation.

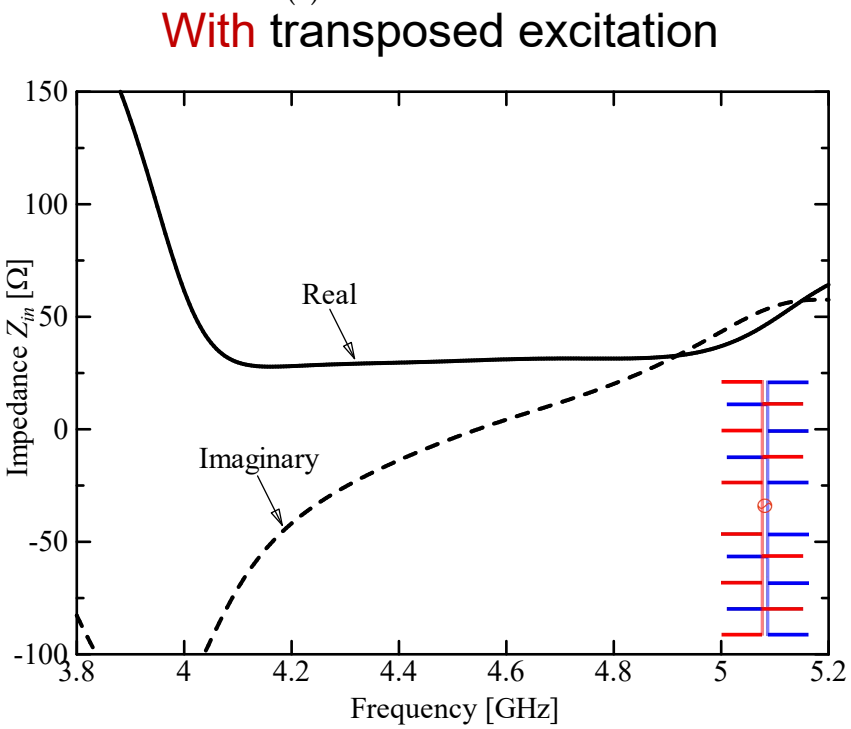

(b) Transposed excitation.

Figure 2.16: Impedance of the series-fed dipole arrays.

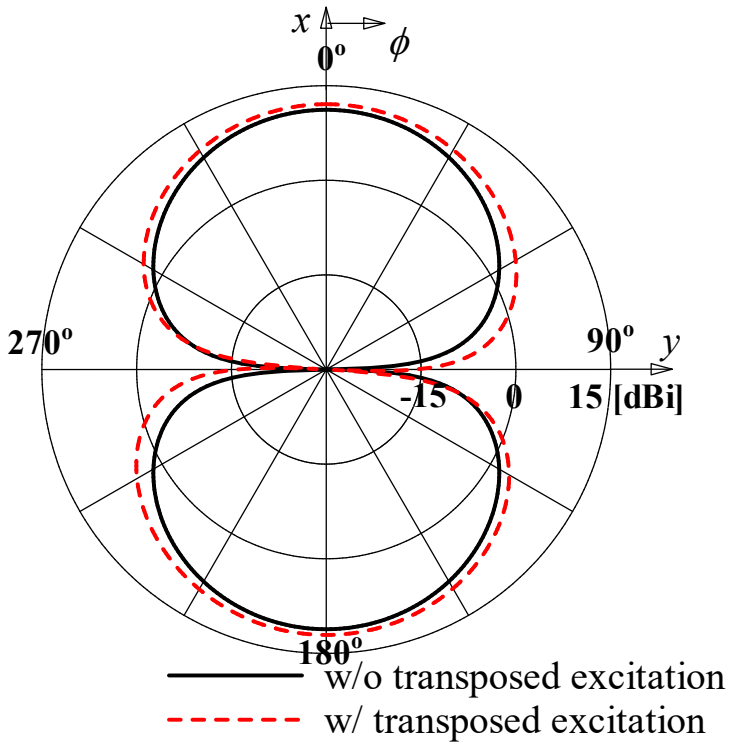

(a) Radiation pattern.

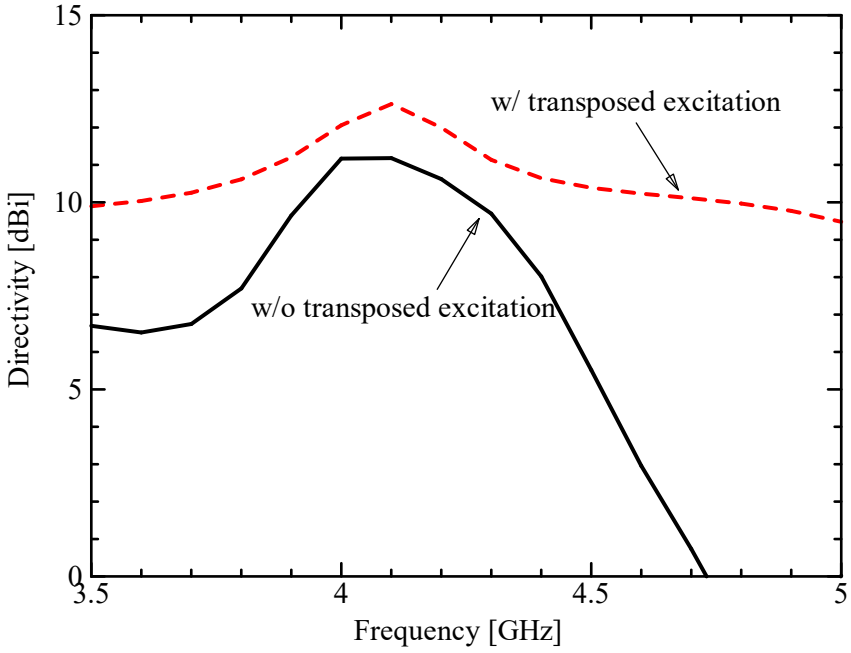

(b) Directivity.

Figure 2.17: Radiation characteristics in horizontal plane.

2.4 Summary

In this chapter, two methods were proposed to achieve broadband performance in series-fed dipole arrays.

The first method involved the implementation of a series-fed non-uniform dipole array. This configuration significantly increased the gain bandwidth compared to uniform array antennas. By using the same non-uniform array, it was also verified to exhibit bandwidth spreading in omnidirectional antenna applications.

The second method introduced a transposed excited series-fed dipole array. By utilizing transposed excitation, the impedance characteristics of the dipole array underwent smooth changes, resulting in improved broadband performance. The 3 dB gain bandwidth of the transposed excited array was extended, showcasing its ability to operate over a wider frequency range.

Both methods presented in this chapter demonstrate effective approaches to achieving broadband properties in series-fed dipole arrays. And they contribute to the development of broadband antenna design techniques.

Chapter 3

A Novel Feeding Method of Broadband Series-fed Antenna for Omnidirectional Radiation Pattern

In this chapter, a novel feeding method inspired by the turnstile antenna is proposed to address these limitations. The proposed antenna design eliminates the need for power dividers and instead utilizes a single port. Despite the simplified feeding structure, the antenna still achieves an omnidirectional radiation pattern with broadband coverage.

3.1 Feeding Methods of Turnstile Antenna

A turnstile antenna, or crossed-dipole antenna, is a radio antenna consisting of a set of two identical dipole antennas mounted at right angles to each other and fed in phase quadrature; the two currents applied to the dipoles are 90 degree out of phase [38].

Specialized turnstile antennas called super turnstile or batwing antennas are used as television broadcasting antennas. We have discussed the advantages and applications of super turnstile in Chapter 1. Fig. 3.1 illustrates the configuration of two crossed half-wavelength dipoles that are energized with currents of equal magnitude but with a 90-degree phase difference, resulting in a four-leaf clover radiation pattern. One of the challenge is how to achieve and the desired 90-degree phase difference.

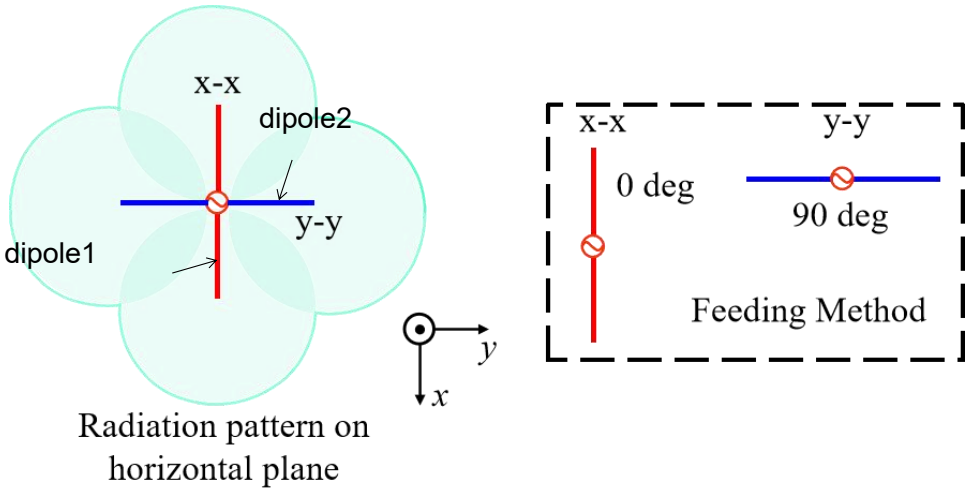

Figure 3.1: The principle of turnstile antenna.

3.1.1 Common Methods of 90 Degree Phase Realization

There are several common methods to achieve a 90-degree phase difference in this scenario [39]. One approach shown in Fig. 3.2(a) is to connect the half-wavelength dipoles to separate transmission lines of unequal lengths. By adjusting the lengths of the transmission lines, the signals traveling through them experience a phase shift, resulting in the desired phase difference between the dipoles. However, it is important to note that this implementation is relatively simple but limited to narrowband oper-

ation. Another method shown in Fig. 3.2(b) involves introducing reactance in series with one of the dipoles. This can be achieved by modifying the physical parameters of the dipole, such as altering its length or diameter. By introducing reactance, the electrical characteristics of the cross dipoles are altered, leading to a phase difference between the two dipoles. However, similar to the previous method, this approach is also relatively simple but typically limited to narrowband applications.

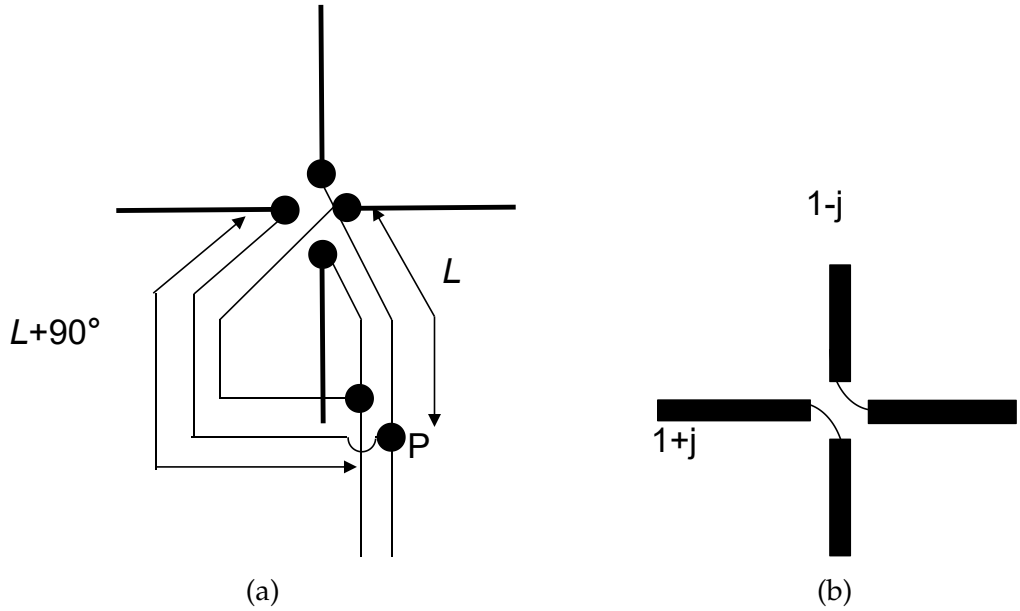

Figure 3.2: The most common ways for 90 degree phase difference.

3.1.2 Actual Feeding Example

In practical applications, the feeding of turnstile antennas often involves connecting two jumpers through a power divider which is shown in Fig. 3.3. In order to achieve high gain by establishing array, multiple power dividers are required. However, this approach can lead to increased costs and bulkiness of the system, making it less suitable for compact base station applications.

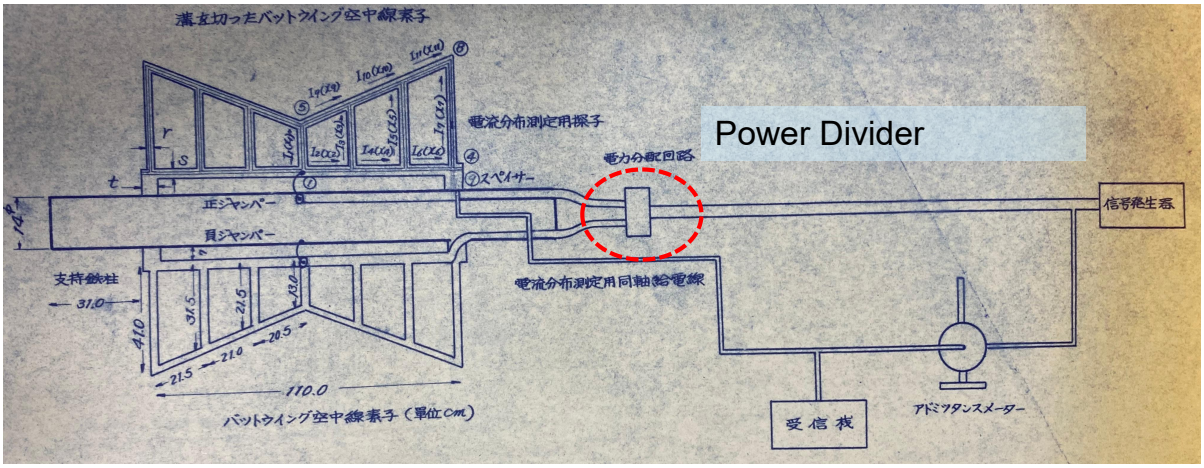

Figure 3.3: Actual feeding method of super turnstile antenna.

3.2 A Novel Feeding Method of Broadband Series-fed Antenna

Conventional turnstile antennas achieve a 90-degree phase difference by using multiple feed lines [13, 16–19] or adjusting the length of crossed dipoles [40]. We would like to apply the turnstile feeding method to a series-fed antenna array. The series-fed dipole array needs only one port in the center to realize the excitation of all units, which effectively reduces the trouble of requiring many cables or power dividers in the practical implementation of turnstile array. The key to the study is how to realize the 90 degree phase difference of crossed dipoles in the series-fed array.

3.2.1 Modified Turnstile Feeding

Fig. 3.4 presents a method to achieve a 90-degree phase difference in series-fed array by using only one port. Instead of relying on multiple ports or power dividers,

this approach utilizes transmission line theory to achieve the desired phase difference.

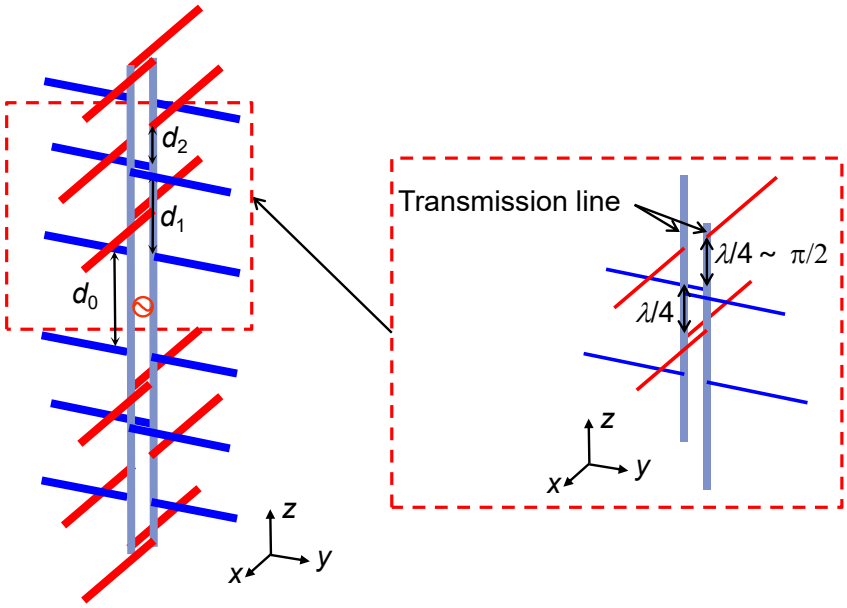

Figure 3.4: Unit configuration with 90 degree phase difference.

By employing a quarter-wavelength transmission line, which introduces a 90-degree phase change, the necessary phase difference can be achieved. The crossed dipoles are then positioned at a distance equivalent to a quarter wavelength. This configuration ensures that the 90-degree phase change occurs between the two crossed dipoles, meanwhile all of the cross dipoles with 90 degree phase difference can be excited by single port.

This method offers a simple and efficient solution for achieving the desired phase difference without the need for additional ports or power dividers. By leveraging the properties of transmission line theory and carefully positioning the crossed dipoles, the 90-degree phase difference can be realized, facilitating the desired radiation pattern and performance.

3.2.2 Modified Transposed Excitation

Broadband performance is achieved through the utilization of the self-complementary cross dipole structure, as discussed in Chapter 2. In this structure shown in Fig. 3.5, the arms of adjacent dipole elements on each plane are swapped, resulting in a 180-degree phase change. Additionally, by placing adjacent elements in the same plane at a distance of half a wavelength apart, another 180-degree phase change is introduced. Thus, in-phase radiation of the elements on the same plane can be achieved, enabling the generation of a high-gain radiation pattern.

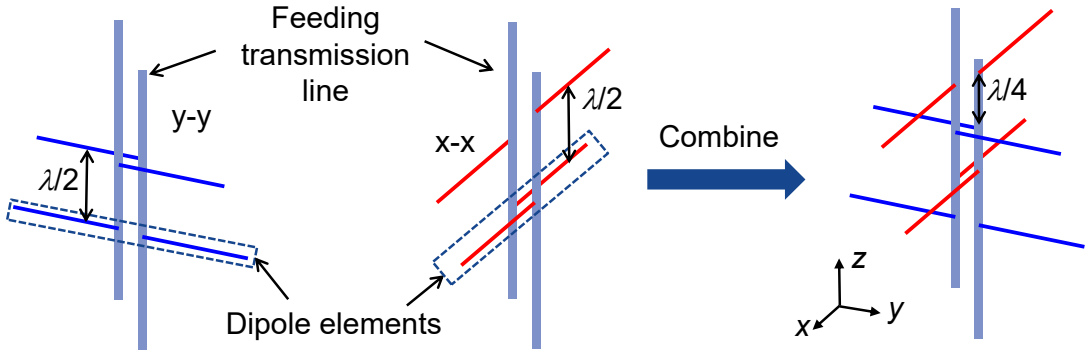

Figure 3.5: Unit configuration with transposed excitation for broadband.

The concept of swapping the arms and maintaining a specific distance between adjacent elements allows for broadband property. It also allows the unit spacing to be shorted from one wavelength to half a wavelength, which can effectively reduce the radiation in the overhead direction and focus the energy on the horizontal plane where we desire.

3.2.3 Antenna Parameters and Properties

Fig. 3.6 shows the overall structure of the antenna. The antenna consists of six pairs

of crossed dipoles, each with a length of $\lambda/2$. These crossed dipoles are connected by transmission lines, utilizing only one port. The arms of adjacent elements within each pair of crossed dipoles are swapped, enabling the desired phase changes. In Fig. 3.6, a pair of crossed dipoles is presented in different colors, indicating a separation distance of $\lambda/4$. On the other hand, identical elements are represented in the same color, achieving a separation distance of $\lambda/2$. Table 3.1 displays the specific parameter values associated with the antenna design.

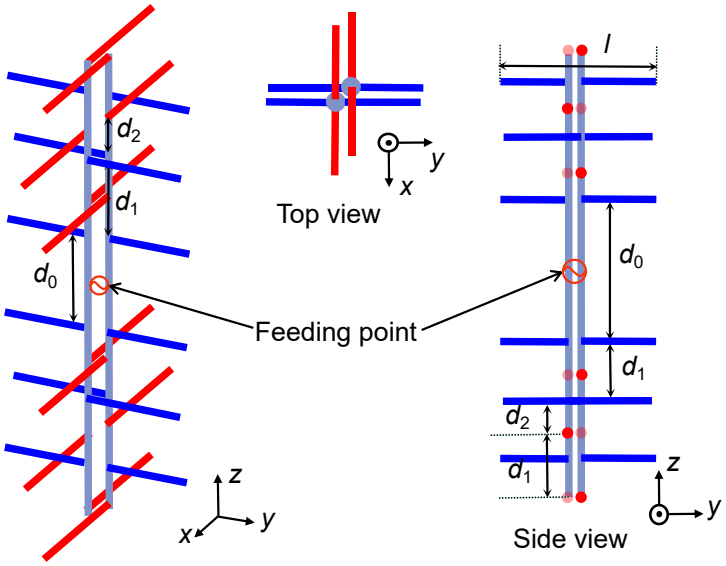

Figure 3.6: Overall geometry of the broadband series-fed dipole array.

The proposed antenna is centrally fed and designed to operate at a frequency of 4 GHz. With its unique configuration, the antenna array is capable of radiating an omnidirectional radiation pattern over a broadband range. Furthermore, the compact size of the antenna makes it suitable for various applications where space constraints are a consideration.

Fig. 3.7 displays the impedance characteristics of the proposed antenna. The real

Table 3.1: The parameters of the broadband series-fed dipole array.

Prameters	Description	Value (mm)
l	Length of dipole element	37.5
d_0	Distance between center elements	50
d_1	Distance between elements in same plane	37.5
d_2	Distance between elements in different plane	18.75

part of the impedance exhibits stability within the frequency range of 4-5 GHz and remains close to 50 ohms. The imaginary part of the impedance changes smoothly across the frequency range and approaches 0. This indicates that the antenna can well match with the standard 50 ohm system, ensuring efficient power transfer and minimizing reflection losses.

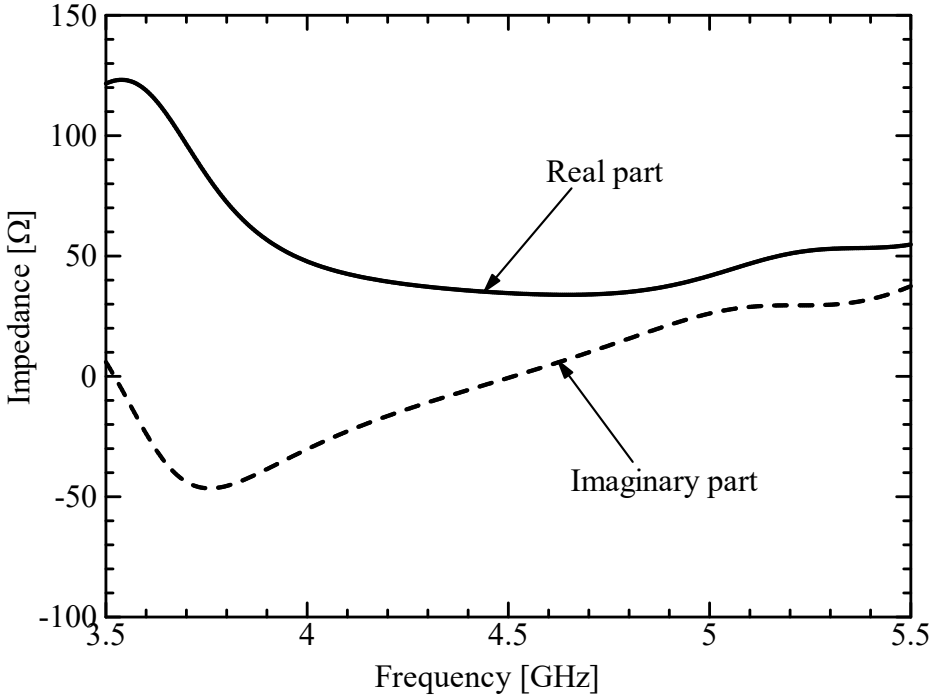

Figure 3.7: Impedance property of proposed antenna.

It is important to notice that the spacing between the dipole elements closest to the feeding point, denoted as d_0, plays a significant role in the impedance matching of the proposed dipole array. The presented Fig. 3.8 shows the reflection coefficient varies with d_0. It becomes apparent that as the value of d_0 increases, the operating frequency of the dipole array shifts towards the lower frequency band. This implies that adjusting d_0 can be used as a means to tune the operating. Furthermore, while the impedance bandwidth of the dipole array experiences slight variation with changes in d_0, it consistently remains above 1 GHz. This suggests that the impedance bandwidth remains almost stable with adjustments to d_0.

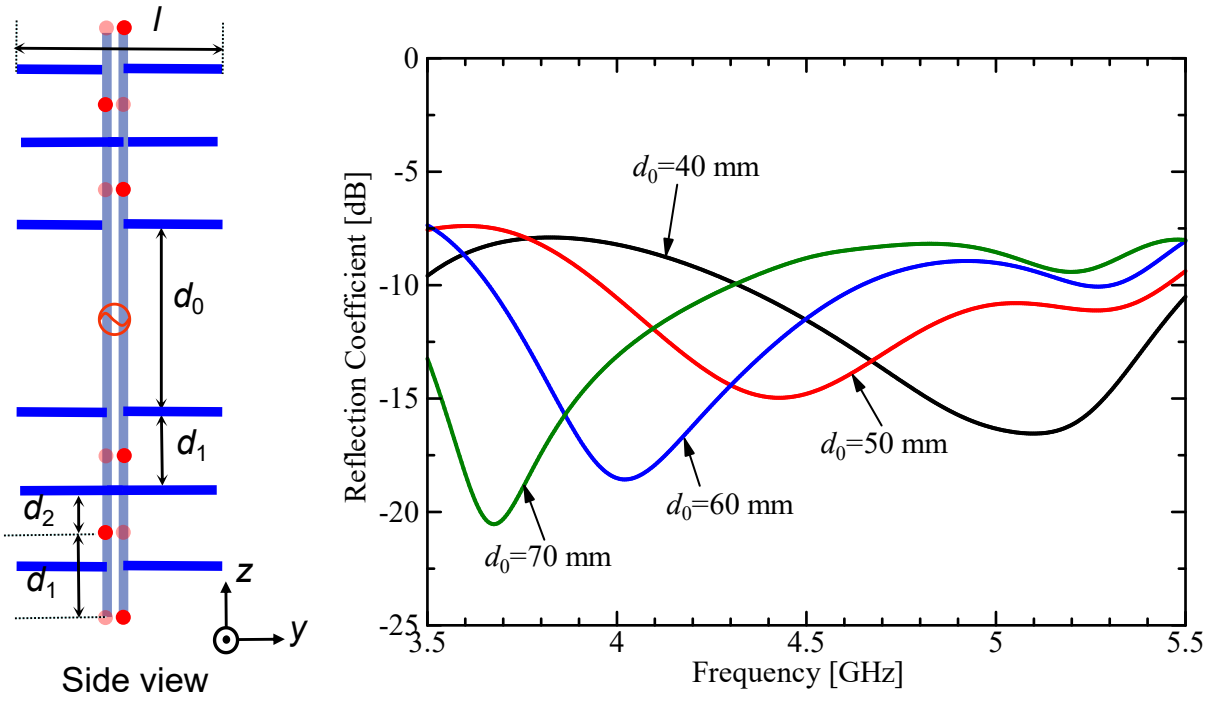

Figure 3.8: Reflection coefficient with different d_0.

The radiation pattern of the proposed antenna is also influenced by the spacing parameter d_0, as demonstrated in Fig. 3.9, showing the radiation patterns in both

horizontal and vertical planes at 4 GHz. In horizontal plane, the radiation pattern mostly maintains a four-leaf clover shape across different values of d_0. However, there is a slight change in the maximum gain. In vertical plane, the radiation pattern changes with d_0 increases. Specifically, the sidelobes and overhead radiation in vertical plane tend to increase.

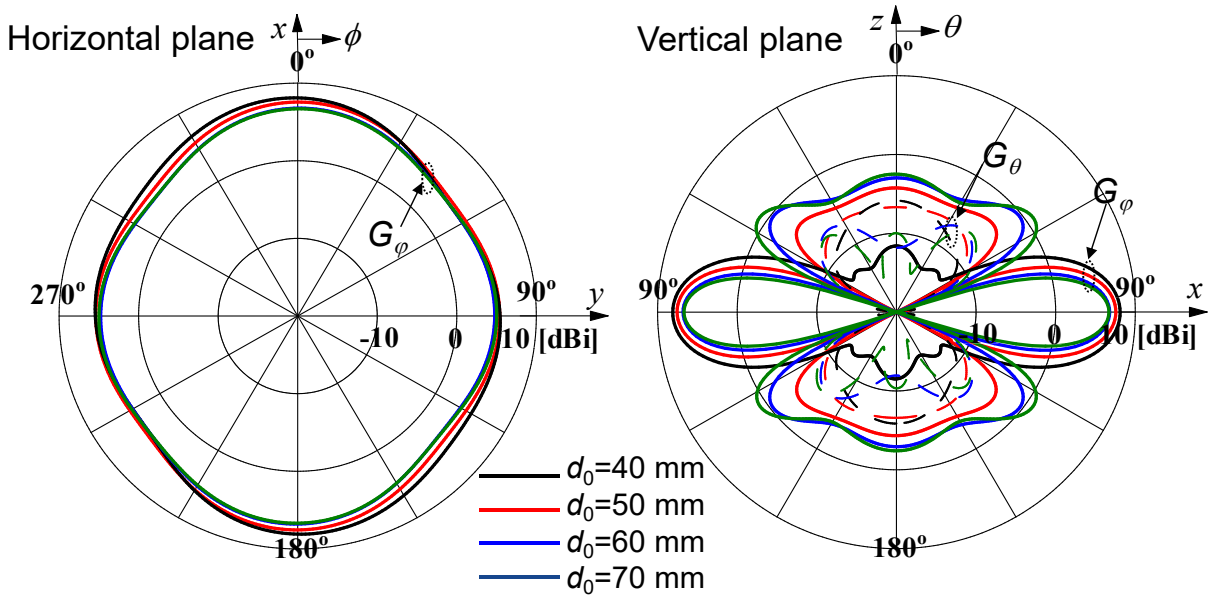

Figure 3.9: Radiation patterns with different d_0.

When selecting the appropriate value for d_0, it is crucial to consider both the requirements for impedance matching and the desired radiation pattern. Simultaneously, it should be balanced with the desired radiation characteristics, including the shape of the radiation pattern and the levels of sidelobes and overhead radiation.

The mean gain, or average gain, provides a comprehensive evaluation method for omnidirectional antennas by considering the gain across the azimuth plane. Unlike the maximum gain, which only represents the highest gain value, the mean gain is calculated by averaging the gains in all directions, taking into account the overall gain in

the desired plane. Some researchers also use roundness to judge the omnidirectional antenna. roundness expresses the difference between the maximum gain and the minimum gain in the desired plane. Compared with this, the average gain is more objective and comprehensive in evaluating the gain level of omnidirectional antenna.

In Fig. 3.10, the relationship between the average gain and frequency is depicted. It can be observed that the maximum value of the average gain is 5.7 dBi, which occurs at 4.7 GHz. Within the frequency range of 4-5 GHz, the average gain exhibits a smooth variation, indicating a broadband property of the antenna.

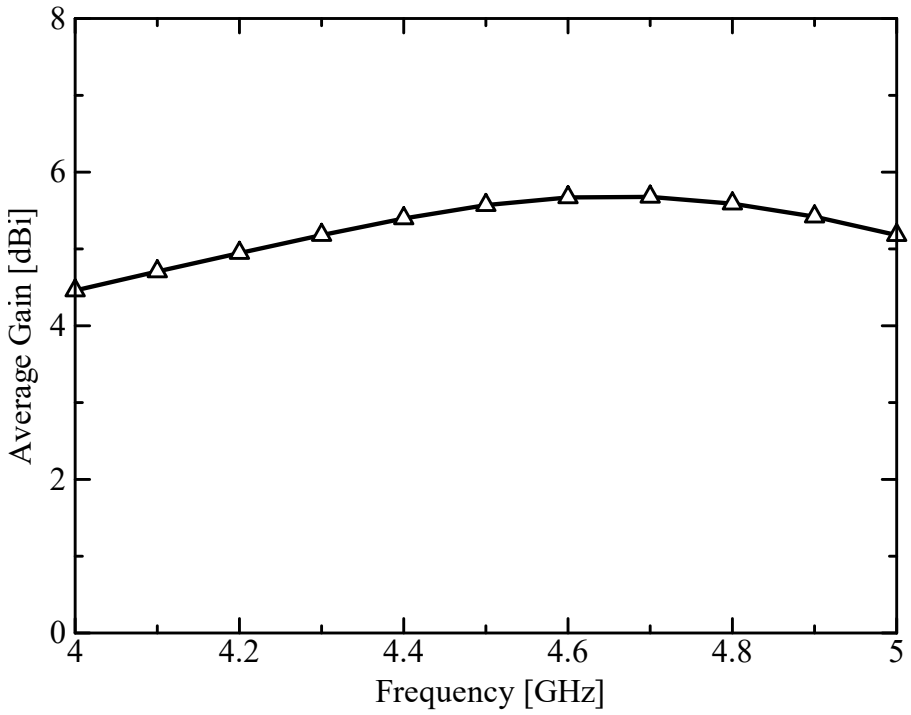

Figure 3.10: Average gain in horizontal plane.

3.2.4 Antenna Processing and Measurement

The proposed antenna is made of 1 mm diameter copper wire and excited by a coaxial line in Fig. 3.11. The experimental setup for evaluating the proposed antenna via a 2-port VNA (Anritsu MS46122B), shown in Fig. 3.12. The proposed antenna is placed on the turntable. A standard horn antenna is used as the receiving antenna. To reduce cable losses, the VNA is placed in an electromagnetic anechoic chamber covered with absorbing material.

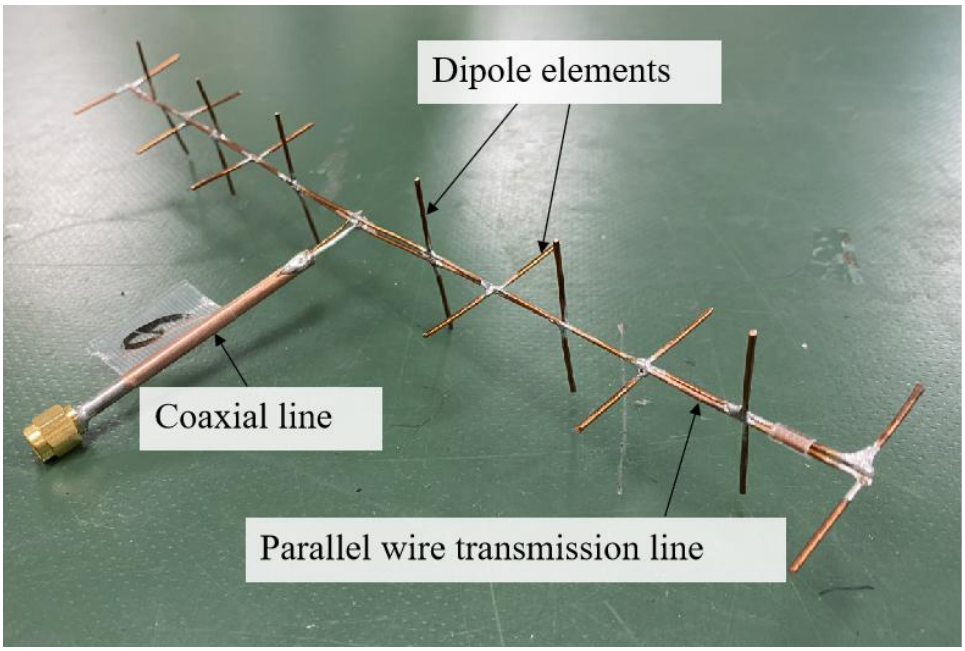

Figure 3.11: Fabrication of the proposed antenna.

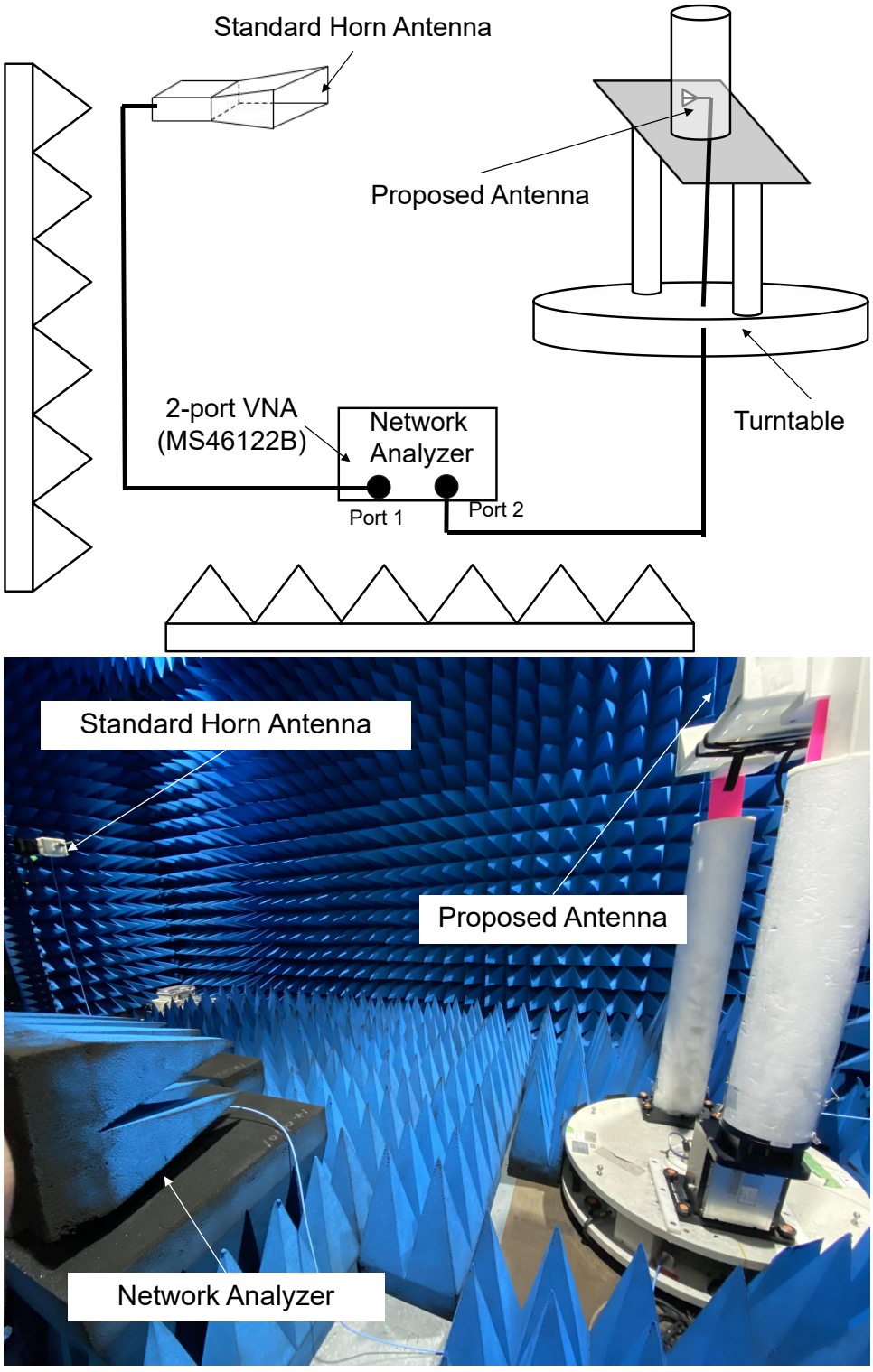

Figure 3.12: Experimental setup.

Fig. 3.13 illustrates the reflection characteristics and realized gain of the antenna. The red line represents the measured results, while the blue line represents the simulated results. The measured 10 dB impedance bandwidth spans from 3.83 to 5.02 GHz, resulting in a relative impedance bandwidth of 26.89%. The measured maximum peak realized gain (RG) is 7.44 dBi, which occurs at 4.4 GHz. Furthermore, the peak realized gain within the 1 dB bandwidth is approximately 22%. It demonstrates the antenna's ability to maintain a relatively high gain over a significant portion of its operating frequency range.

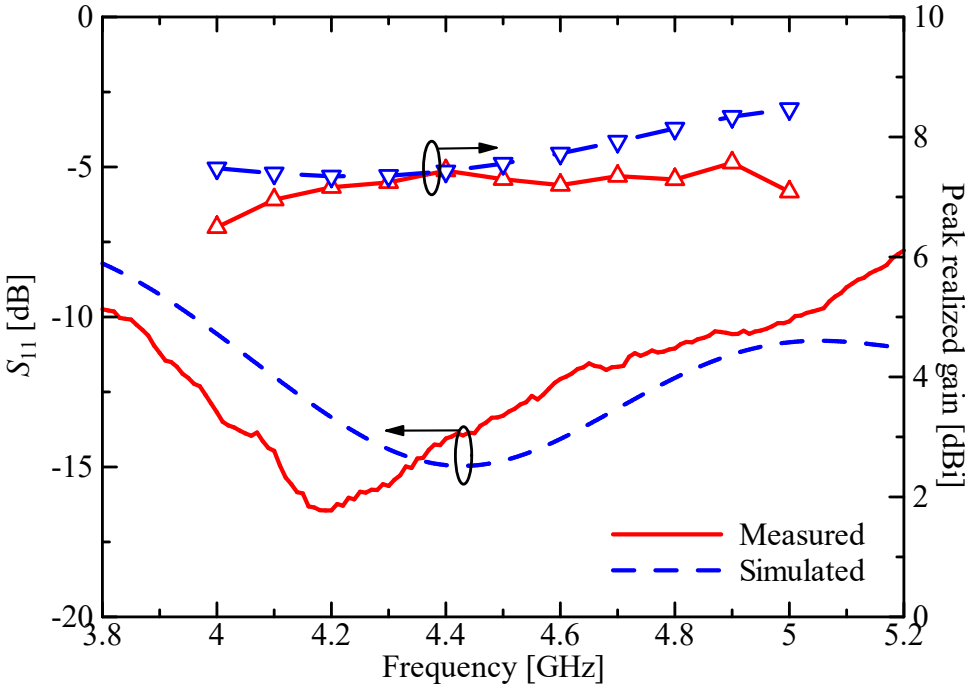

Figure 3.13: Reflection characteristics and realized gain.

The experimental and simulated results depicted by the red and blue lines respectively exhibit good agreement, indicating a close correlation between the measured and predicted performance of the antenna.

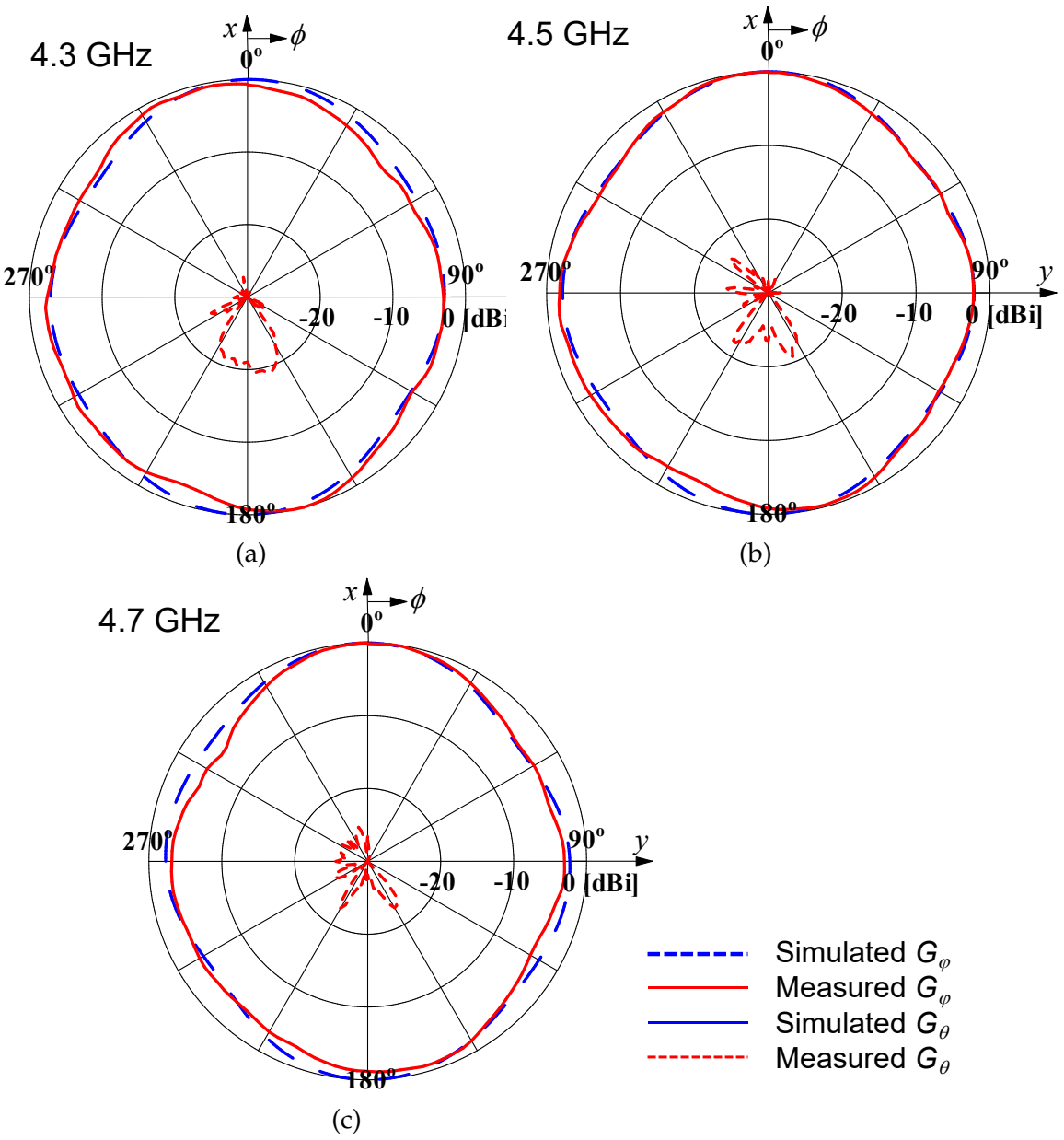

Figure 3.14: Normalized radiation patterns at different frequencies.

Fig. 3.14 depicts the radiation patterns of the antenna at different frequencies. The radiation patterns obtained from measured results and simulated results are com-

pared, and a good agreement between the two is observed. However, it is worth noting that there is a slightly larger error at high frequencies.

The discrepancy between the measured and simulated results at high frequencies can be attributed to several factors, with the main contributor being the hand-made. Whether the position and angle of the units are accurate in the processing will affect the measured results of the antenna. Especially in the series-fed antenna, the accumulated errors are more obvious in the high frequency band. At the same time, the antenna is made of 1 mm diameter copper wire for the sake of easy soldering, and the material itself is relatively soft, so a slight bending will also lead to the deflection of the radiation patterns.

3.2.5 Performance Comparison with Other Works

Table 3.2 presents a comparison between the proposed omnidirectional horizontally polarized dipole array and previous works, highlighting key parameters and information for a clear assessment. In terms of bandwidth, the proposed dipole array outperforms previous works. For instance, the achieved 22% bandwidth surpasses the 7.3%, 8%, and 3.7% bandwidths reported in [41], [42], and [32], respectively. Moreover, the design presented in [30] achieves a comparable bandwidth of 34%. However, it is important to note that this design has a substantially longer structure, which may pose challenges in terms of size constraints and practical implementation. In contrast, the proposed dipole array achieves a high bandwidth while maintaining a more compact size. Additionally, the RG per unit length is an important parameter to consider. The proposed design demonstrates a higher RG per unit length (2.4 dBi) compared to the value reported in previous works (1.13 dBi). This indicates that the proposed OHP dipole array achieves higher gain efficiency in terms of the amount of gain obtained

per unit length of the antenna.

Table 3.2: Performance comparison of high gain omnidirectional horizontally polarized antenna arrays.

Ref.	Freq (GHz)	BW (%)	Max cross-section area (λ^2)	Peak RG (dBi)	RG per unit length (dBi/λ)
[9]	1.67-2.27	34	7.11×1.11	8	1.13
[10]	2.35-2.55	7.3	6×0.23	9.7	1.61
[11]	9.6-10.4	8	4.3×0.22	10.4	2.42
[12]	2.41-2.5	3.7	2.95×0.31	8.52	2.89
Our work	4-5	22	3.17×0.5	7.44	2.35

3.3 Summary

In this chapter, a novel feeding method was proposed for achieving a broadband series-fed antenna with an omnidirectional radiation pattern, taking inspiration from the turnstile antenna concept. According to transmission line theory, the 90 deg phase difference was achieved by putting the crossed dipoles at a distance of a quarter wavelength. The antenna design ensured a compact form with a maximum cross-section area of $3.17 \times 0.5\lambda^2$, which could be confined within a cylinder. This compact size facilitated by using a 1 mm diameter copper wire, and the antenna was fed through a coaxial structure positioned at the center of the array. Experimental measurements demonstrated an impressive -10 dB impedance bandwidth of 1.19 GHz, ranging from 3.83 to 5.02 GHz, accounting for a relative bandwidth of 26.89%. The peak realized gain (RG) value measured at the desired frequency was 7.44 dBi, indicating excellent radiation performance. Furthermore, the proposed antenna exhibited a 1 dB gain

bandwidth of 1 GHz (22%), spanning from 4 to 5 GHz, indicating its capability to maintain a high gain over a wide frequency range.

Chapter 4

Omnidirectional Circularly Polarized Series-fed Antenna Array

In recent years, the role of satellite communications in 5G/Beyond 5G has been attracting attention, and activities of European projects and standardization have been progressing. In light of this situation, circularly polarized (CP) antennas, as the main means of satellite communication, will be more often used in base station antennas. Meanwhile, omnidirectional circularly polarized (OCP) antennas are also ideal for applications in Internet-of-Things (IoT) system, personal devices, and 5G communications [43–46]. This chapter discusses the OCP, series-fed antenna.

4.1 Previous Studies of OCP Antennas

The Lindenblad antenna, which Nils Lindenblad created for the Radio Corporation of America (RCA) in the early 1940s, may be the first omnidirectional CP antenna [47]. Electric and magnetic radiating components are frequently used to create OCP. Arc

dipoles [48–51] or slits [52–54] are employed to create magnetic components, whereas top-load monopoles are frequently utilized as electric radiators. Fig. 4.1 shows a classic example by using monopole and loop to generate CP fields [55]. The impedance bandwidth is 13 MHz (1429–1442 MHz), and the peak gain is 1.01 dBic. In addition, dielectric resonator antennas (DRA) excited by LP antennas can also be converted to CP antennas [56, 57]. In [57], CP field is obtained by introducing several inclined slits to the sidewalls of the rectangular dielectric resonator antenna, the degeneracy mode is excited to generate the circularly polarized (CP) fields in Fig. 4.2. But both of them have a shortcoming of low gain which is not suitable for base station cases.

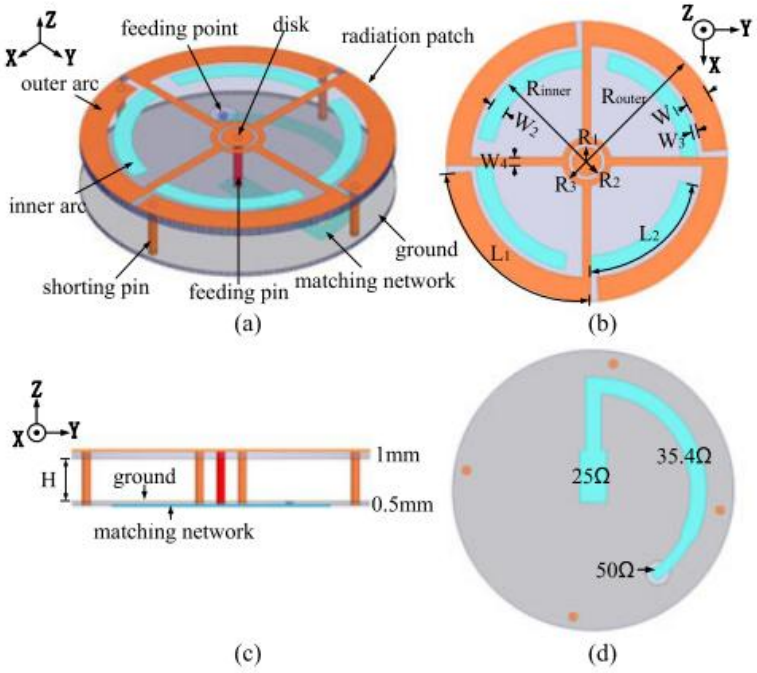

Figure 4.1: Previous studies of realization on circularly polarized antennas using monopole and loop [55].

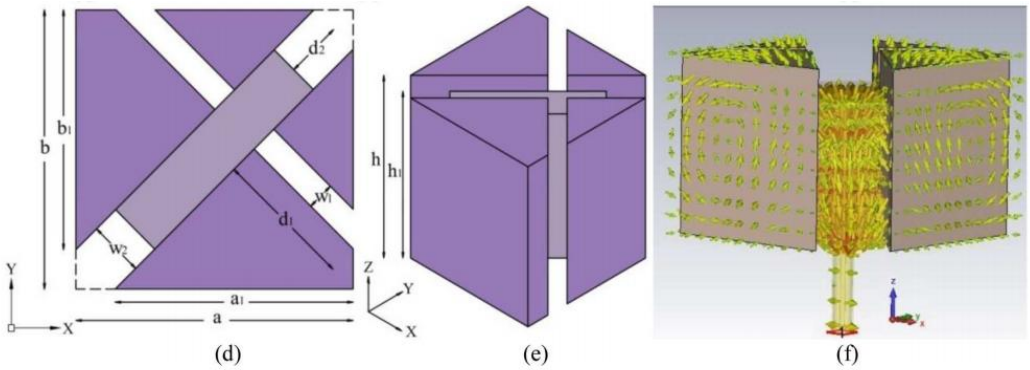

Figure 4.2: Previous studies of realization on circularly polarized antennas using slit inclined DRA [57].

There are only a few researches on OCP Antenna Arrays with high gain. In Fig. 4.3, the antenna array comprises four identical circularly polarized (CP) antenna elements, intricately interconnected through a parallel strip-line feeding network [58]. Each CP antenna element encompasses a dipole and a zero-phase-shift (ZPS) line loop, ingeniously harnessed to generate vertically and horizontally polarized omnidirectional radiation, respectively. Notably, the vertically polarized dipole is strategically positioned within the center of the horizontally polarized ZPS line loop. The maximum gain of 5.4 dBic is achieved. Another one is formed by cascading several stages of electric (metallic strips) and magnetic (loops) radiators into a highly compact array [59]. In Fig. 4.4, five E-radiators and six M-radiators are excited to generate circularly polarized (CP) fields. A measured maximum realized gain of 7.1 dBic with a bandwidth covers 2.37–2.48 GHz.

Both designs achieve high gain, but the design of [17] is more compact than [16], which does not require a complex feed network, making it more suitable for use in miniaturized base stations. In this chapter, this design will be studied based on this design.

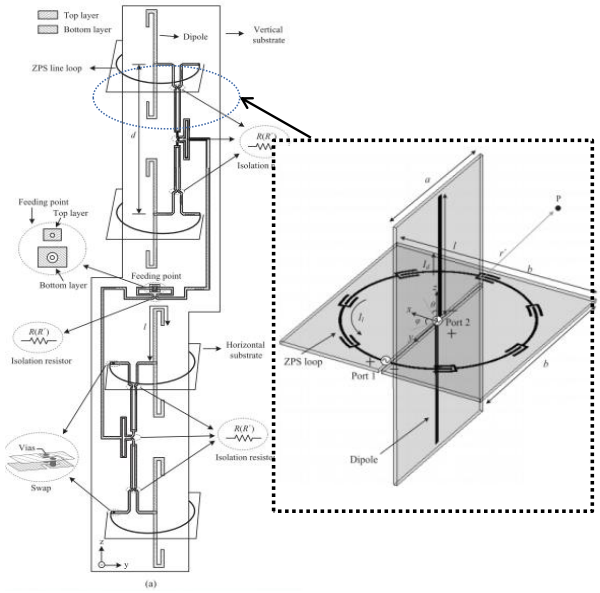

Figure 4.3: Previous studies of realization on circularly polarized antennas using dipole and ZPS loop array [58].

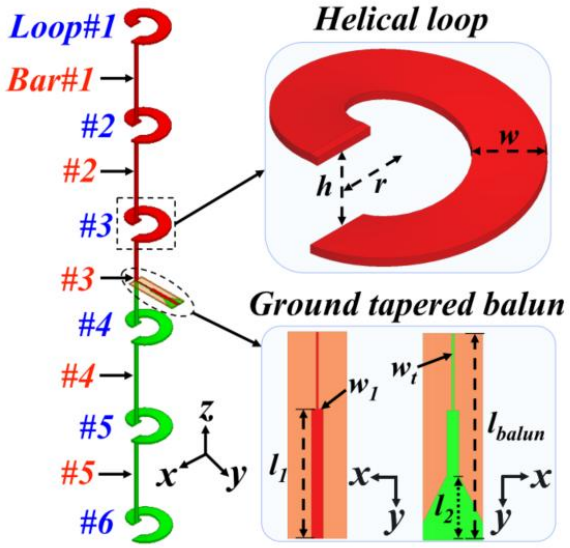

Figure 4.4: Previous studies of realization on circularly polarized antennas using collinear high gain array with loops and strip bars [59].

4.2 Theory of OCP Series-fed Antenna Array

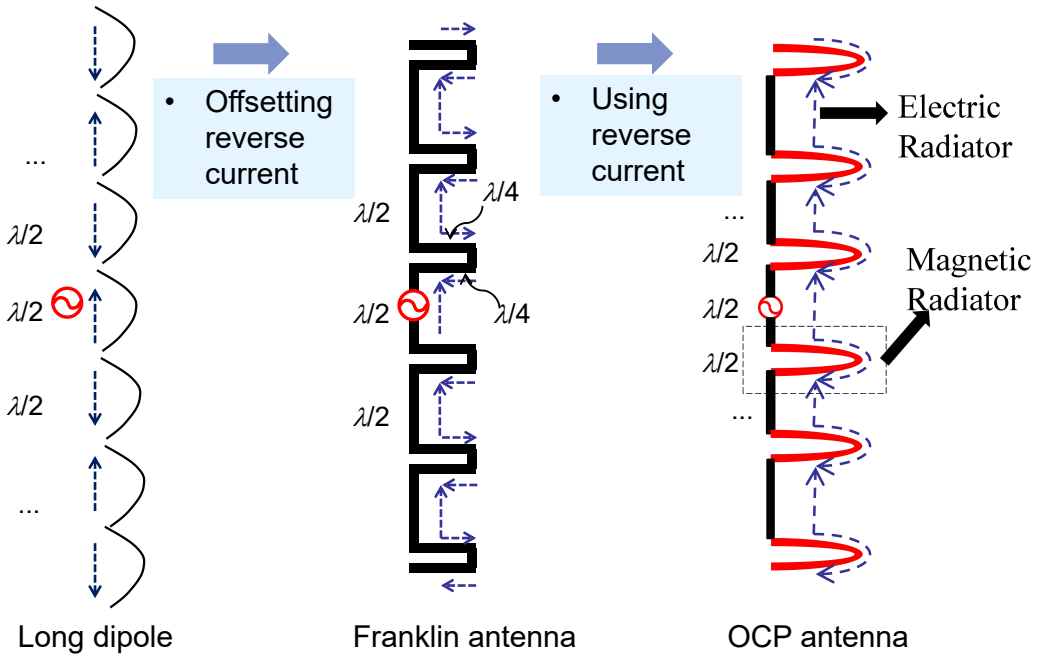

Figure 4.5: Current distribution of the antenna.

In Fig. 4.5, an elucidation of the current distribution of the antenna elements is presented, shedding light on their intricate workings. Firstly, a comprehensive depiction of the current distribution for long dipole is illustrated, demonstrating the periodic reversal of current along its length, occurring precisely at intervals of half a wavelength. Secondly, an exploration into the Franklin antenna reveals a captivating phenomenon where the generation of reverse current induces a bending effect, resulting in the cancellation of said current and the subsequent emergence of vertically oriented currents of same phase alignment. Conversely, the proposed antenna design harnesses the potential of the reverse current by ingeniously transforming it into a loop antenna as a magnetic radiator for horizontal polarization, thus enabling the emission of in-phase

radiation. In this condition, the strip parts and the loop parts are in phase, respectively. However, it is imperative to note that within this innovative design, the length of each dipole unit and loop remains constant at precisely half a wavelength, showcasing the intricacies and limitations of this captivating configuration.

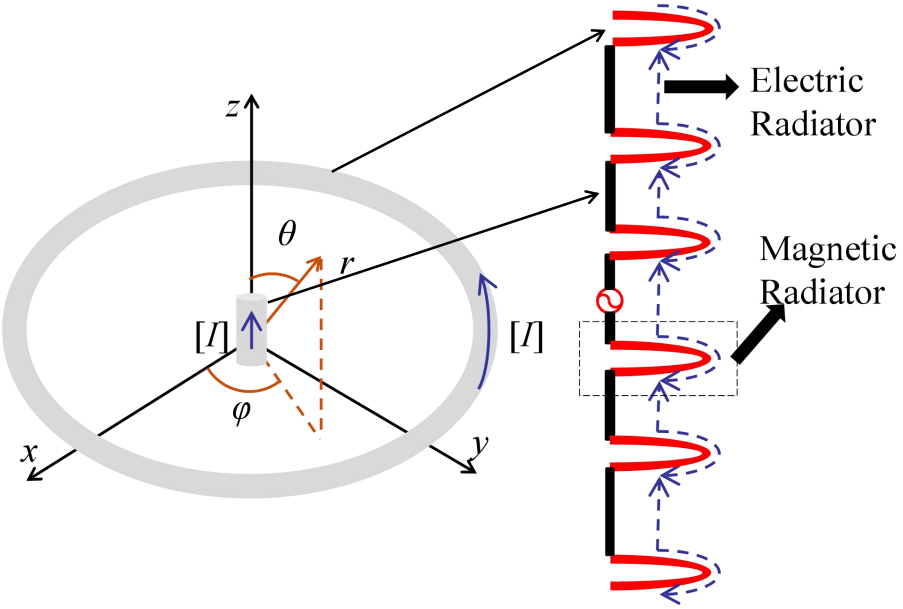

Figure 4.6: Principle of CP fields generation.

The fundamental method of this CP antenna is a combination of dipole and loop which is shown in Fig. 4.6. Polarization of dipole and loop are orthogonal, providing the possibility to realize CP. Same amplitudes of E_θ and E_ϕ can be obtained by adjusting the current distributions on the two elements, resulting in a good CP property. The half-wavelength straight section, depicted here in black, which functions as a vertically polarized (VP) electric dipole radiator. In stark contrast, the ingenious inclusion of a helical loop, distinguished by its red color, is strategically positioned between two electric dipole sections. The flow of currents, denoted by the blue dashed line.

It is crucial to note that the attainment of a high-performance CP antenna necessitates a delicate balance between the two orthogonal components. Specifically, these components should exhibit equal amplitudes and a precise phase difference of 90 degrees. However, this pursuit of perfection presents its own set of challenges and complexities, warranting further investigation and consideration.

4.3 Defects in Antenna Structure

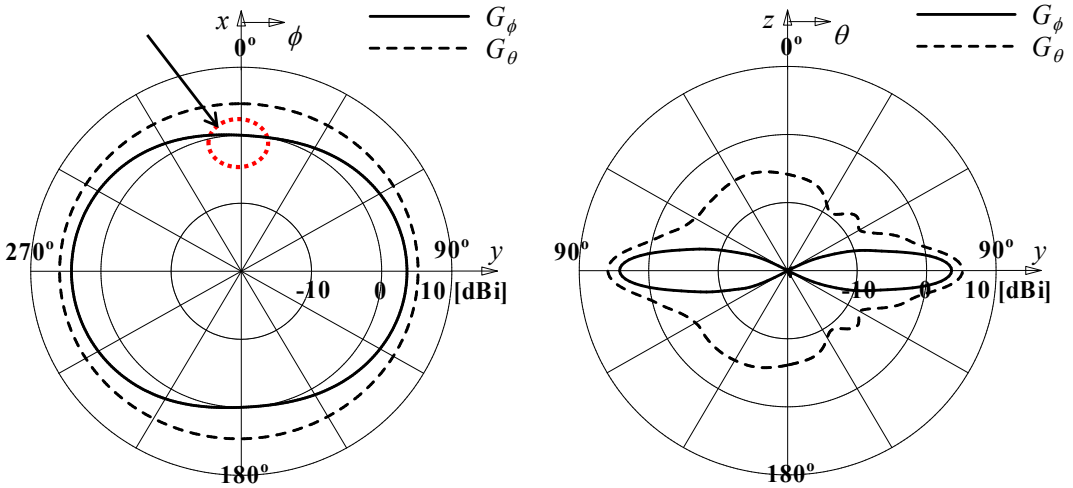

Figure 4.7: Linear polarized (LP) radiation patterns (ten-stage).

Under this antenna operating mechanism, the length of the electric and magnetic radiators is fixed. This leads to limitations in forming circular polarization. These problems can be seen in LP radiation patterns of the ten-stage OCP array depicted in Fig. 4.7. Notably, a discernible deficiency arises in the phi-component radiation pattern around the angle of ϕ=0 degrees, resulting in a deviation from the desired omnidirectional pattern. Additionally, both in the horizontal and vertical planes,

the ϕ-component of gain exhibits a relatively lower magnitude compared to the θ-component. These two issues collectively contribute to a less favorable CP property, posing challenges in achieving the desired circular polarization characteristics. Addressing these limitations becomes imperative to enhance the overall performance and effectiveness of the OCP array.

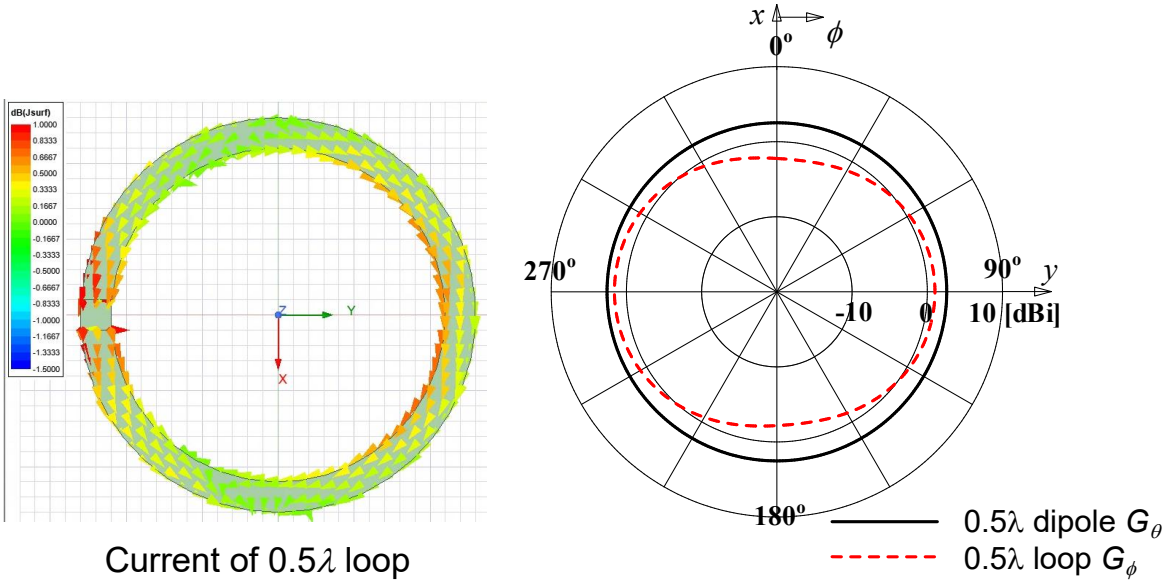

(a) Current distribution of half wavelength loop.

(b) Radiated ability of half wavelength dipole and loop.

Figure 4.8: The reason for poor CP characteristic.

The underlying reasons behind the aforementioned limitations are elucidated in Fig. 4.8. Upon examining the current distribution on the half-wavelength loop, a non-uniform pattern is discernible. The radiation pattern of the half-wavelength loop, as depicted by the red line in Fig. 4.8(a), further highlights this non-uniformity. This non-uniform current distribution poses the first challenge, as it disrupts the desired omnidirectional characteristics of the ϕ-component radiation in Fig. 4.8(b). Moreover, comparing the radiation patterns of the half-wavelength loop and the half-

wavelength dipole antenna, depicted by the red and black lines respectively, a notable disparity becomes apparent. The dipole antenna exhibits a higher radiation intensity in comparison to the loop antenna. In the proposed series-fed CP antenna array, this discrepancy between the electric and magnetic radiators' radiation capabilities contributes to a undesirable gain for the CP antenna as a whole.

Taken together, these factors significantly impact the CP characteristics of the antenna, leading to subpar performance. Addressing these concerns becomes crucial in order to enhance the overall CP performance and achieve the desired circular polarization properties.

4.4 Multi-side OCP Antenna Array

In order to address one of the problems, which stems from the non-uniform currents on the loop and results in a compromised omnidirectional radiation pattern, we propose a solution. To mitigate the impact of non-uniform currents, we suggest orienting the open-ends of the loops in different directions.

The configuration of the multi-side OCP antenna is illustrated in the accompanying Fig. 4.9. In this arrangement, each loop is rotated counterclockwise by an angle determined by the given equation, with the n-th loop serving as the reference. The parameter m represents the number of variations in the loop directions. It is important to note that the antenna array exhibits rotational symmetry along the y-axis.

For demonstration purposes, the upper half of a ten-stage multi-side OCP antenna array is shown in Fig. 4.9(b). Specifically, the arrangement of the 1-side and 4-side OCP antennas is depicted. The 1-side case represents the original structure described in the referenced paper, while the 4-side OCP antenna showcases the implementation of a proposed orientation of the loop open-ends.

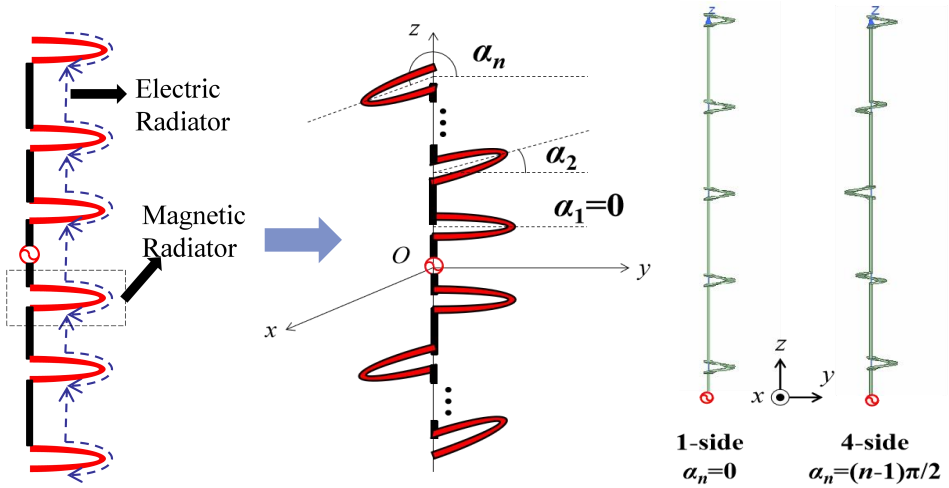

(a) Antenna construction.

(b) Configurations of 1-side and 4-side cases.

Figure 4.9: Ten-stage multi-side OCP antenna array.

Fig. 4.10 presents the LP and CP radiation patterns in the horizontal plane of the 4-side OCP antenna. A comparison is made between the 4-side array and the 1-side array to assess the improvements achieved. In the case of the 4-side OCP antenna, the inclusion of additional sides results in a more omnidirectional phi-component generated by the loops. Consequently, in the CP radiation pattern, the roundness, which represents the deviation from perfect circular polarization, is effectively suppressed to less than 1 dB. This enhancement signifies a improvement over the performance of the 1-side array.

The roundness of the proposed antenna is shown in Fig. 4.11. The results reveal that the 4-side arrangement exhibits significantly lower roundness values in the frequency range of 3.5 GHz to 4.3 GHz, as compared to the 1-side case. In fact, the roundness remains consistently below 1 dB, indicating a high degree of circular polarization and thus a favorable omnidirectional performance.

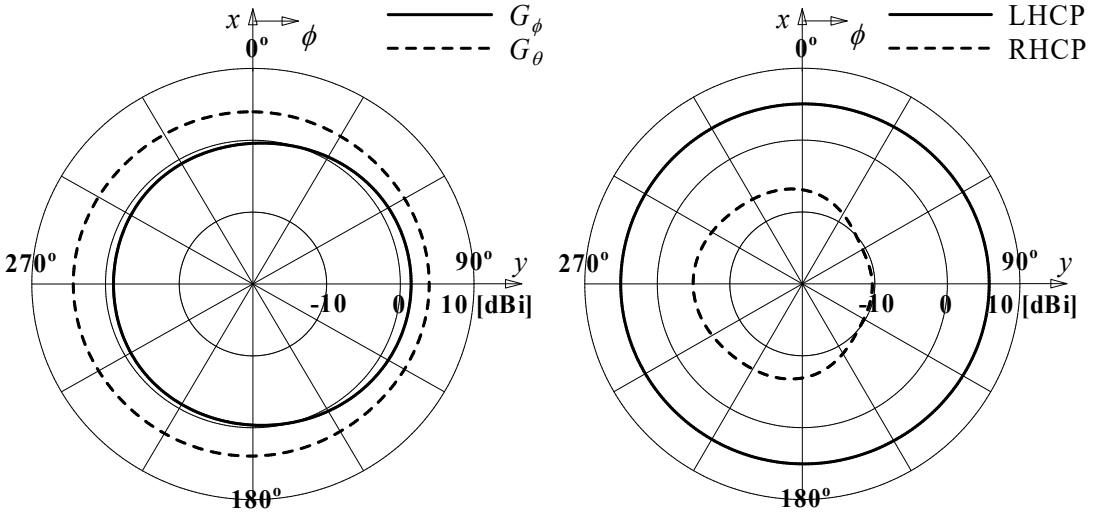

(a) Linearly polarized(LP) radiation pattern.

(b) CP radiation pattern.

Figure 4.10: Radiation patterns of 4-side OCP antenna array.

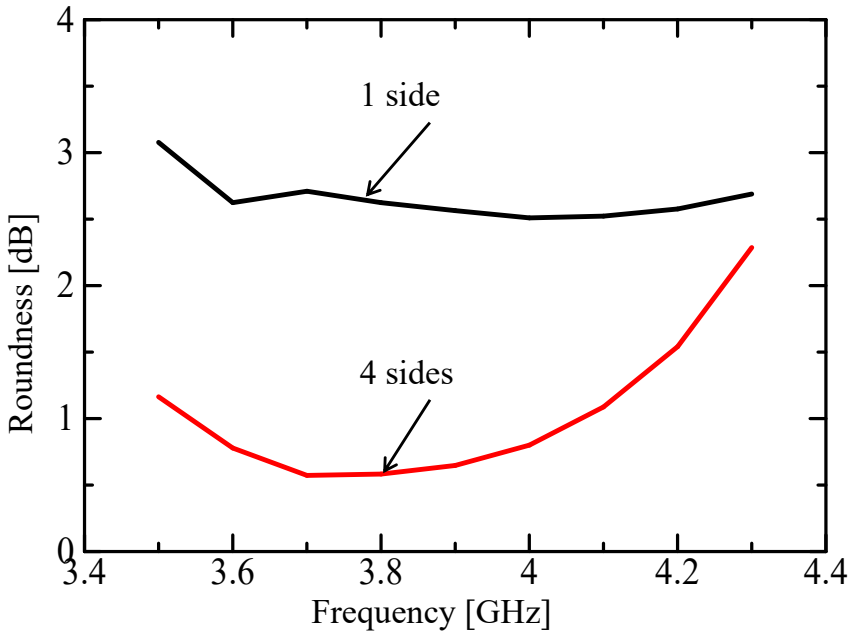

Figure 4.11: Roundness of 4-side OCP antenna array.

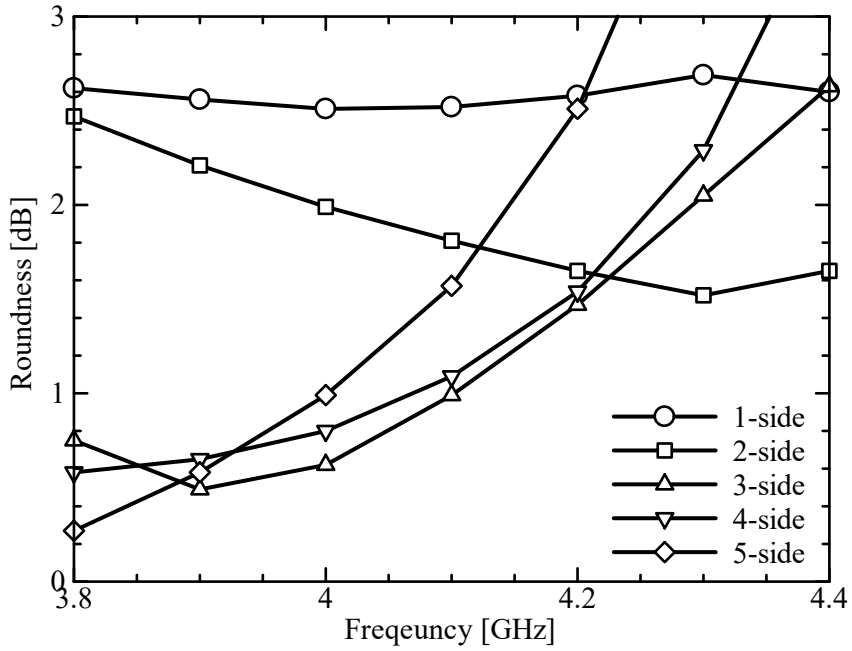

(a) Roundness.

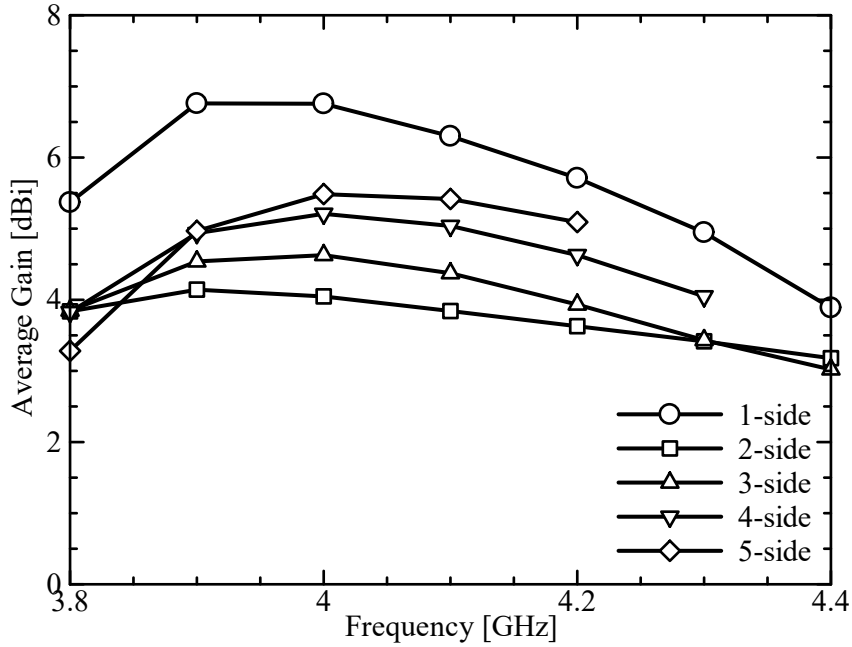

(b) Average gain.

Figure 4.12: Roundness and average gain of multi-side OCP antenna array.

Fig. 4.12 presents the roundness and average gain of multi-side OCP antenna arrays. Different lines represent different multi-side arrangements, each characterized by a specific number of orientations m. The results clearly demonstrate that the multi-side arrangement offers the potential for improved omnidirectional performance. When the number of orientations m exceeds 3, the roundness of the antenna can be effectively suppressed below 1dB, resulting in a desirable omnidirectional performance. However, it should be noted that while better roundness has been achieved at 4 GHz with the multi-side OCP antenna, the roundness may deteriorate when considering a larger bandwidth.

In Fig. 4.12(b), only the frequencies that meet the roundness requirement are plotted. It can be observed that the average gain of the multi-side OCP antenna array decreases compared to the 1-side case. However, the average gain shows an increasing trend as the rotation direction number m increases.

4.5 Center Loop Loaded OCP Antenna Array

In this part, we present a proposal aimed at addressing the issue of a weaker ϕ-component compared to the θ-component, which results from the disparities in radiation ability between the electric and magnetic radiators in the antenna array.

To enhance the ϕ-component, we introduce a loop in the center of the array. This loop serves to augment the radiation in the desired direction. The upper half of the center loop loaded OCP antenna array is depicted in Fig. 4.13. By strategically placing the loop in the center, we aim to achieve a more balanced radiation pattern with improved ϕ-component characteristics.

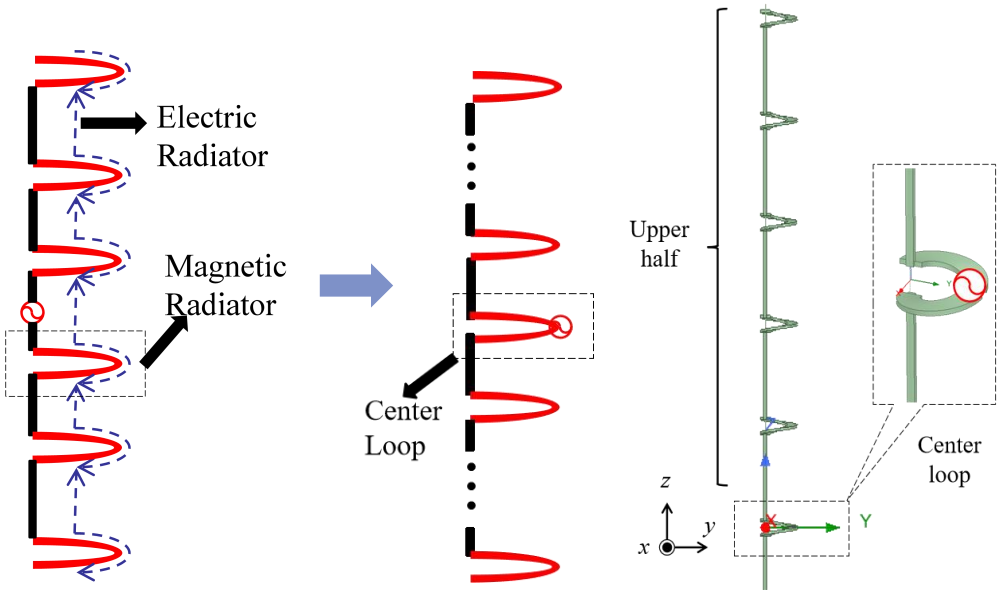

(a) Antenna construction.

(b) Upper half of 10-stage center loaded OCP antenna array.

Figure 4.13: Center loaded OCP antenna array.

Fig. 4.14 presents the radiation patterns in the horizontal plane at 4 GHz for the proposed center loop loaded OCP antenna array. In LP radiation pattern, it is evident that the ϕ-component has been significantly enhanced in all directions compared to the previous configuration. This enhancement results from the addition of the center loop, which effectively strengthens the radiation in the ϕ direction. As a result, the antenna exhibits improved performance in terms of the LP radiation pattern. Furthermore, the incorporation of the center loop has also led to a better CP property. This improvement is reflected in the CP radiation pattern, where the gain levels are more balanced between the θ and ϕ components. The achieved better CP gain level highlights the effectiveness of the proposed approach in enhancing the circular polarization characteristics of the antenna.

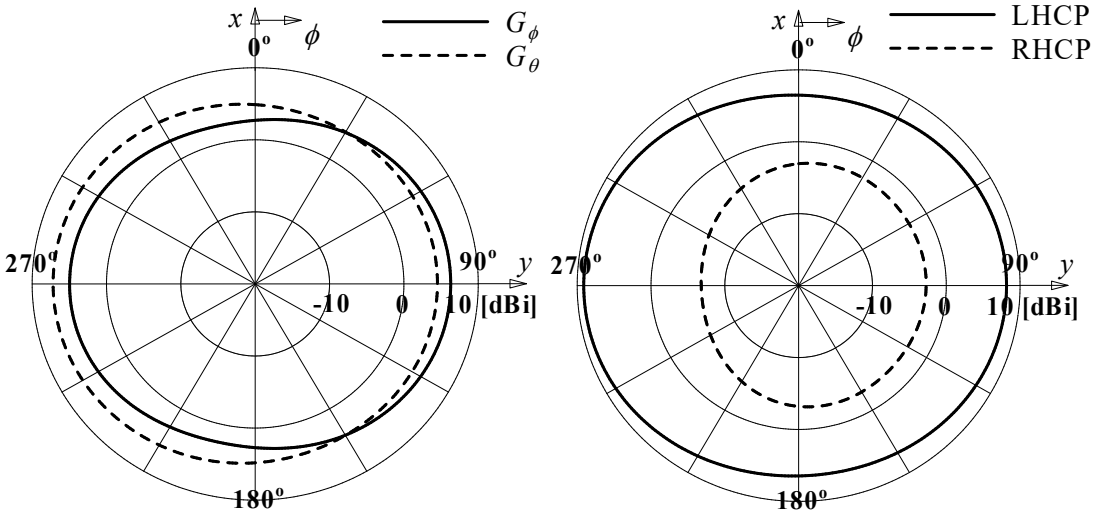

(a) LP radiation pattern. (b) CP radiation pattern.

Figure 4.14: Radiation patterns of center loaded OCP antenna array.

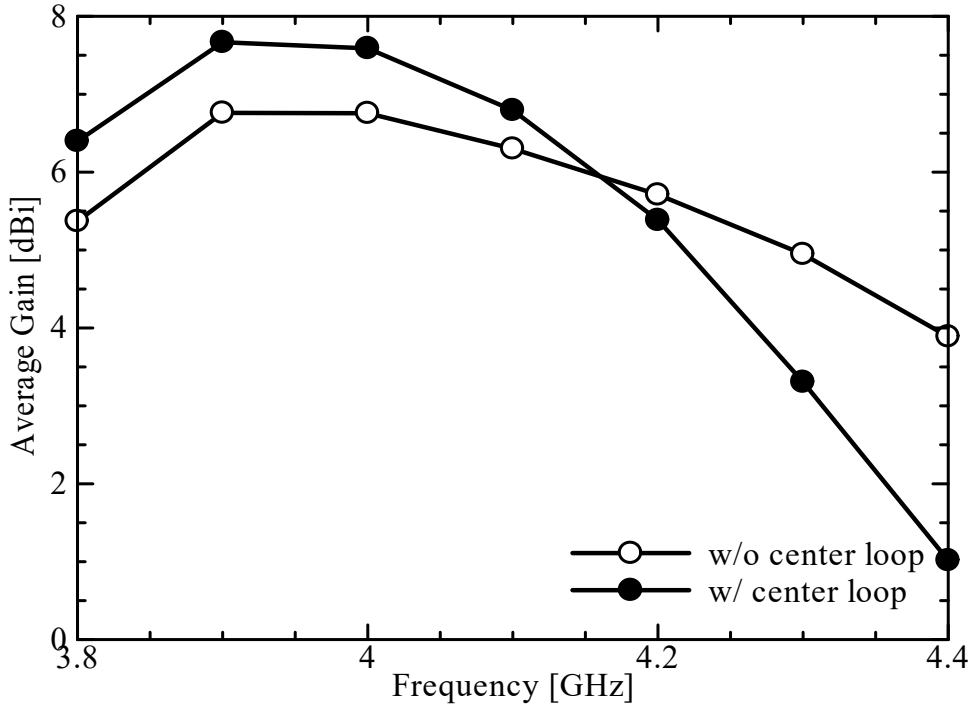

Figure 4.15: Average gain of center loaded OCP antenna array.

The average gain of the proposed antenna is presented in Fig. 4.15. By adding the center loop, there is a significant improvement in the average gain level within the frequency range of 3.8-4.1 GHz. This enhancement indicates the effectiveness of the center loop in boosting the overall gain performance of the antenna. However, it should be noted that the addition of the center loop also leads to a narrowing of the average gain bandwidth. While the average gain is improved within a specific frequency range, the overall bandwidth over which the antenna operates at high gain levels becomes more limited.

This trade-off between gain improvement and bandwidth narrowing should be carefully considered when designing and selecting the antenna configuration, taking into account the specific requirements and priorities of the application.

4.6 Summary

In this chapter, In this chapter, we presented the methods to achieve omnidirectional circularly polarized (OCP) antennas with both omnidirectional radiation properties and better CP property. The goal was to address two key challenges: improving the non-omnidirectional pattern caused by non-uniform currents in half-wavelength loops and enhancing the radiation efficiency of the magnetic radiator for increased gain.

Firstly, we introduced a technique to adjust the open-end orientations of the loops. This adjustment significantly improves the non-omnidirectional pattern resulting from non-uniform currents in the half-wavelength loops. By carefully manipulating the orientations, we have achieved a remarkable enhancement in the omnidirectional radiation pattern.

Furthermore, we proposed the integration of a center loop in the OCP antenna array. This addition effectively enhanced the radiation capabilities of the magnetic radiator,

leading to improved CP property. The center loop plays a crucial role in enhancing the f-component and achieving a higher level of CP gain. The results demonstrated that the maximum CP gain reached to 9.02 dBic at 4 GHz.

The methods presented in this chapter provide valuable insights into the design and optimization of OCP antennas with enhanced omnidirectional properties and better CP property. These advancements have the potential to greatly benefit various applications that require reliable and efficient wireless communication systems.

Chapter 5

Conclusions

In this dissertation, a comprehensive exploration of series-fed antenna technology was conducted, with a focus on the development of omnidirectional base station antennas suitable for Sub-6 frequencies in the context of 5G/B5G communications. The research aimed to address the challenges of achieving compact size, cost-effectiveness, wide bandwidth, and simple feeding techniques. Additionally, circularly polarized series-fed antennas were investigated to enable polarization diversity.

Chapter 1 served as an introduction, providing a background to the research and highlighting the antenna requirements and challenges in the 5G/B5G era. The importance of addressing these challenges was emphasized, laying the foundation for the subsequent chapters.

Chapter 2 delved into the enhancement of bandwidth for series-fed antennas. The dissertation first introduced the series-fed antenna technique, along with its application scenarios, advantages, and limitations. While the series-fed antenna offers simplicity and cost advantages, it suffers from narrow bandwidth. To overcome this limitation, two design methods for broadband antennas were proposed. The first method

involved designing a non-uniform series-fed antenna array based on the principle of multiple resonant antennas, resulting in significantly improved gain bandwidth. The second method proposed a transposed excited series-fed dipole array inspired by self-complementary antenna principles, which exhibited stable impedance and radiation patterns over a wide frequency band, thereby achieving broadband characteristics. These approaches presented valuable insights and methodologies for achieving bandwidth spreading in series-fed antennas.

Chapter 3 introduced a novel feeding method for omnidirectional series-fed broadband dipole array antennas. Drawing inspiration from the feeding technique of the turnstile antenna, the dissertation proposed a design that achieved omnidirectional radiation by strategically arranging the dipole units and feeding them through a single port. Experimental results confirmed that the antenna, processed with a 1mm copper wire and fed through a coaxial structure in the center, achieved an impressive 10 dB impedance bandwidth of 26.9% (3.83-5.02 GHz). The measured maximum gain reached 7.44 dBi, with a 1 dB gain bandwidth of 22%. The experimental and calculated results exhibited good agreement, showcasing the feasibility of the proposed series-fed broadband omnidirectional antenna design.

Chapter 4 focused on the omnidirectional circularly polarized series-fed array antenna. Taking a high-gain omnidirectional series-fed circularly polarized antenna structure as an example, the chapter addressed the inherent limitations of the structure, namely the poor omnidirectional radiation characteristics of the phi component and differences in radiation between orthogonal components. To enhance the circular polarization characteristics, two improvement proposals were presented. Firstly, by rotating the open-end direction of the loop unit, the roundness of the antenna was improved. Secondly, the addition of a loop unit at the center of the array enhanced loop radiation, leading to improved circular polarization characteristics, specifically

reflected in the enhancement of circular polarization gain. These proposals demonstrated significant effects in achieving uniform radiation and enhancing circular polarization characteristics, making them highly valuable for practical applications in circularly polarized series-fed base station antennas.

Chapter 5 served as the concluding chapter, summarizing the key findings and contributions of the dissertation.

In the future, how to further improve the omnidirectional property of the series-fed dipole array is a topic that needs to be further studied. At the same time, whether applying the non-uniform array mentioned in Chapter 2 to the transposed excited array proposed in Chapter 3 can further improve the bandwidth of the series-fed antenna is also worthy of further discussion.

In summary, this dissertation offers valuable insights and methodologies for the design and optimization of series-fed antennas, the outcomes of this research significantly contribute to the performance enhancement and feature expansion of next-generation mobile communications, as well as the development of electromagnetic wave engineering and communication engineering.

Acknowledgments

This dissertation summarizes the work during my Ph.D. life. Throughout the process of preparing data and writing this thesis, I gradually realized that the numerous attempts I made over the past four and a half years were all meaningful. Half a year ago, I did not dare to think about these.

I deliberately placed the acknowledgment section in the last part to write because its writing style and mental feeling differ completely from the preceding parts. It mirrors the most genuine me, a highly sensitive and empathetic girl. The latter part may be very long.

I would prefer to describe these five years of my Ph.D. program as five years of living in Japan. I have experienced the challenges of research, met various individuals, tried many new things, and addicted to a couple of delicious food. Despite the difficulties, I never lacked satisfaction and happiness.

First, I would like to express my sincere gratitude to Prof. Noriharu Suematsu, Prof. Hiroki Nishiyama, and Prof. Keisuke Konno for their valuable advice and suggestions on my research. I am also grateful for their kindness and encouragement, which make me confident during my nervous presentation.

In September 2015, I met Prof. Qiang Chen for the first time and knew about the student exchange program at Tohoku University. Prior to that, I had never considered

studying abroad, let alone pursuing a Ph.D. The language barrier and unfamiliar environment filled me with fear, but my curiosity for new experiences gave me a nudge. I am thankful to Prof. Chen for granting me that opportunity, which exposed me to a broader world. Besides knowledge, I am fortunate that Prof. Chen taught me the right attitude toward scientific research. Rather than focusing solely on optimizing parameters to perfection, understanding the principles behind them is the most valuable and challenging aspect. Maintaining a sincere pursuit of the essence of truth is precious not only for researchers but also in a society that tends to prioritize results in this rapidly evolving world. Furthermore, I appreciate Prof. Chen's tolerance and encouragement, especially during times when my papers faced repeated rejections.

I am deeply grateful to Prof. Qiaowei Yuan. She exemplifies the strength of women in engineering through her actions and serves as a role model for me. I will always remember her words, "You can come to me for any difficulties you encounter, whether in research or life." She is like a family member or close friend. Make me know that whenever I face challenges, she stands behind me, providing support and guidance.

I extend my thanks to Ms. Yumiko Ito for assisting with various complex procedures and occasionally sharing Japanese snacks with me.

I would like to express my gratitude to those who helped me during my master's exchange period. Thank you to Prof. Hiroyasu Sato for teaching me the basics of lens design and experimental methods. I am grateful to Dr. Yang Li for his support in both research and life. Thanks to Yiwen Zhu for his assistance with the Japanese language. I appreciate the company of Lifei Zheng. I am also grateful to Prof. Yu Tan and Cheng Wang for helping me acclimate to the unfamiliar environment. Likewise, thank you to Lingqian Wang, Muyi Li, Xuhong Sun, and the warm-hearted people who made me feel welcome in Sendai. It is because of all of you that I was determined to continue my Ph.D. studies in Sendai.

Thank you to my boyfriend, Junyi Xu, for accompanying me through the ups and downs, sharing laughter and tears, enjoying delicious food together, staying up late for experiments, and writing papers. He has been the strongest support in my Ph.D. life. Every late-night snack we had together made me feel a bit guilty but incredibly happy. Of course, we both gained weight. I hope that we can continue to excel in our respective fields, encourage each other, and also be childish and understanding in our daily lives. Let's explore more cities, witness more sceneries, and indulge in more delicious food together.

I am grateful to my best friends, Dr. Xianbo Cao, Dr. Ruolin Fu, and Dr. Yuxin Li. I feel incredibly lucky to have met all of you during my Ph.D. journey. I deeply appreciate the support and assistance you provided whenever I faced difficulties. Your sincerity and timely help meant a lot to me. Thank you for sharing both the joys of life and the process of research with me. Your presence made me feel less alone. Special thanks to Shuangyue Xu, a quiet yet warm-hearted girl. I will never forget the memories we shared as "Wu Tiao Ren" and the "The Big Band" in that summer. I would also like to thank Uncle Zhang for sharing his experiences and preparing various delicious dishes. And to Ting Wang, Lin Zhang, Ying Tong, Zhonggen Wang, and Takuma Nakamura, thank you for the fun times we spent together, filled with laughter and jokes. I would also like to thank the understanding and trust of the lab members and friends.

There is another group of people who are in China. I want to thank my parents for their understanding and support. I am grateful for the family atmosphere they created, which allows me to speak my mind without any hesitation. I would also like to thank our family pets, "Luni" and "Meixi," who have accompanied my parents throughout these years. Thank you to my brothers and sisters and my friends in China. Each time they ask, "When are you coming back?" with a hint of complaint, it warms my heart.

They have been a source of strength in my academic journey.

Furthermore, I would like to extend my appreciation to the National Institute of Information and Communications Technology (NICT) for their significant support in this research. I am also deeply grateful for the financial assistance provided by the Japanese Government scholarship during my study and living period in Japan.

Every time I wanted to give up, repeatedly whispered, "Just hold on a little longer," so in the end I want to thank the persistent myself.

July, 2023

Reference

[1] https://www.soumu.go.jp/main_content/000696613.pdf

[2] https://www.titech.ac.jp/news/2023/065654

[3] https://businessnetwork.jp/article/8479/

[4] J.Xu, S. Wu and Q. Chen, "Dual-Band Antennas with High-Gain and Omni-directional Radiation Pattern Enhanced by Single-layer Radome," *IEICE Communications Express*, Vol.X12-B,No.8,pp.-,Aug. 2023.

[5] Bjornson, Emil, et al. "Massive MIMO in sub-6 GHz and mmWave: Physical, practical, and use-case differences." *IEEE Wireless Communications* 26.2 (2019): 100-108.

[6] S. Xia, C. Ge, Q. Chen and F. Adachi, "A Study on User-antenna Cluster Formation for Cluster-wise MU-MIMO," *2020 23rd International Symposium on Wireless Personal Multimedia Communications (WPMC)*, Okayama, Japan, 2020, pp. 1-6.

[7] https://www.softbank.jp/corp/news/press/sbkk/2021/20210714_01/

[8] https://www.eet-china.com/mp/a120592.html

[9] https://www.zhihu.com/question/20304283/answer/24807477

[10] https://en.wikipedia.org/wiki/Batwing_antenna

[11] https://en.wikipedia.org/wiki/Helical_antenna

[12] https://rapidservice.neon.jp/document/nhk-hamamatsutv.htm

[13] Takao Kanai,"The Differences between Broadcasting and Communication about Antenna," *The Journal of IEICE*, Vol.101, No.10, 2018.

[14] Keiji Endo, Yukio Endo, Hirosi Okamura, "Stacked Loop Antenna for UHF-TV Broadcasting," *The journal of the Institute of Television Engineers of Japan*, Vol.18, No.5, 1964.

[15] Bartlett, George W., *National Association of Broadcasters Engineering Manual*, 6th Ed., 1975.

[16] R. W. Masters, "The super turnstile antenna," *Broadcast News*, no. 42, January 1946.

[17] Y. Mushiake, (Ed.) *Antenna Engineeriag Handbook*, The OHM-Sha, Ltd., October, 1980.

[18] G. Sato, H. Kawakami, H. Sato and R. W. Masters, "Design method for fine impedance matching super turnstile antenna and characteristics of the modified batwing antenna," *IEICE Transactions*, vol. E-65, pp. 271-278, May 1982.

[19] H. Kawakami, G. Sato and R. Masters, "Characteristics of TV transmitting batwing antennas," *IEEE Transaction on Antennas and Propagation*, vol. 32, no. 12, pp. 1318-1326, December 1984.

[20] S. Wu, L. Wang, T. Kou and Q. Chen, "Dual-polarized Omni Antenna for Sub6 Base Station," *IEICE Society Conference*, B-1-93, Sept. 2020.

[21] Headland, Daniel, et al. "Tutorial: Terahertz beamforming, from concepts to realizations." *Apl Photonics* 3.5 (2018): 051101.

[22] B. Jones, F. Chow and A. Seeto, "The synthesis of shaped patterns with series-fed microstrip patch arrays," *IEEE Transactions on Antennas and Propagation*, vol. 30, no. 6, pp. 1206-1212, November 1982.

[23] Huang, John. "A parallel‐series‐fed microstrip array with high efficiency and low cross‐polarization." *Microwave and Optical Technology Letters* 5.5 (1992): 230-233.

[24] B. -K. Tan, S. Withington and G. Yassin, "A Compact Microstrip-Fed Planar Dual-Dipole Antenna for Broadband Applications," *IEEE Antennas and Wireless Propagation Letters*, vol. 15, pp. 593-596, 2016.

[25] F. Tefiku and C. A. Grimes, "Design of broad-band and dual-band antennas comprised of series-fed printed-strip dipole pairs," *IEEE Transactions on Antennas and Propagation*, vol. 48, no. 6, pp. 895-900, June 2000.

[26] T. Ma, J. Ai, M. Shen and W. T. Joines, "Design of Novel Broadband Endfire Dipole Array Antennas," *IEEE Antennas and Wireless Propagation Letters*, vol. 16, pp. 2935-2938, 2017.

[27] H. Wang, K. E. Kedze and I. Park, "A High-Gain and Wideband Series-Fed Angled Printed Dipole Array Antenna," *IEEE Transactions on Antennas and Propagation*, vol. 68, no. 7, pp. 5708-5713, July 2020.

[28] H. Wang and I. Park, "Coplanar Strip Line-Fed Series Dipole Array Antenna for High-Gain Realization," *IEEE Transactions on Antennas and Propagation*, vol. 69, no. 8, pp. 5106-5111, Aug. 2021.

[29] N. K. Maurya, M. J. Ammann and P. Mcevoy, "Series-fed Omnidirectional mm-Wave Dipole Array," *IEEE Transactions on Antennas and Propagation*, doi: 10.1109/TAP.2022.3232240.

[30] Xu Lin Quan, Rong-Lin Li, Jian Ye Wang, and Yue Hui Cui, "Development of a Broadband Horizontally Polarized Omnidirectional Planar Antenna and Its Array for Base Stations," *Progress In Electromagnetics Research*, Vol. 128, 441-456, 2012.

[31] N. Nguyen-Trong, T. Kaufmann and C. Fumeaux, "A Wideband Omnidirectional Horizontally Polarized Traveling-Wave Antenna Based on Half-Mode Substrate Integrated Waveguide," *IEEE Antennas and Wireless Propagation Letters*, vol. 12, pp. 682-685, 2013.

[32] Z. Zhou, Y. Li, Y. He, Z. Zhang and P. -Y. Chen, "A Slender Fabry–Perot Antenna for High-Gain Horizontally Polarized Omnidirectional Radiation," *IEEE Transactions on Antennas and Propagation*, vol. 69, no. 1, pp. 526-531, Jan. 2021.

[33] R. C. Dai, H. Su, S. J. Yang, J. -H. Ou and X. Y. Zhang, "Broadband Electromagnetic-Transparent Antenna and Its Application to Aperture-Shared Dual-Band Base Station Array," *IEEE Transactions on Antennas and Propagation*, vol. 71, no. 1, pp. 180-189, Jan. 2023.

[34] L. Mingyun, H. Minjie and W. Zhe, "Design of multi-band frequency selective surfaces using multi-periodicity combined elements," *Journal of Systems Engineering and Electronics*, vol. 20, no. 4, pp. 675-680, Aug. 2009.

[35] K. Raha and K. P. Ray, "Broadband High Gain and Low Cross-Polarization Double Cavity-Backed Stacked Microstrip Antenna," *IEEE Transactions on Antennas and Propagation*, vol. 70, no. 7, pp. 5902-5906, July 2022.

[36] http://www.sm.rim.or.jp/ ymushiak/sub.en.3.htm

[37] http://www.sm.rim.or.jp/ ymushiak/sub.4.htm

[38] https://en.wikipedia.org/wiki/Turnstile_antenna

[39] Kraus, J. D., & Marhefka, R. J. *Antenna for all applications*, McGraw-Hill, 2002, pp. 726-729.

[40] I. Radnović, A. Nešić and B. Milovanović, "A New Type of Turnstile Antenna," *IEEE Antennas and Propagation Magazine*, vol. 52, no. 5, pp. 168-171, Oct. 2010.

[41] Z. Liang, Y. Li, X. Feng, J. Liu, J. Qin and Y. Long, "Microstrip Magnetic Monopole and Dipole Antennas with High Directivity and a Horizontally Polarized Omnidirectional Pattern," *IEEE Transaction on Antennas and Propagation.*, vol. 66, no. 3, pp. 1143-1152, Mar. 2018.

[42] W. Lin and R. W. Ziolkowski, "High-Directivity, Compact, Omnidirectional Horizontally Polarized Antenna Array," *IEEE Transaction on Antennas and Propagation.*, vol. 68, no. 8, pp. 6049-6058, Aug. 2020.

[43] L. J. Ricardi, "Communication satellite antennas," *Proc. IEEE*, vol. 65, no. 3, pp. 356–367, Mar. 1977.

[44] L. Bras, N. B. Carvalho, P. Pinho, L. Kulas, K. Nyka, "A Review of Antennas for Indoor Positioning Systems," *International Journal of Antennas and Propagation*, pp. 1-14, 2012.

[45] S. Yan, P. J. Soh, and G. A. E. Vandenbosch, "Wearable dual-band magneto-electric dipole antenna for WBAN/WLAN applications," *IEEE Transaction on Antennas and Propagation.*, vol. 63, no. 9, pp. 4165–4169, Sep. 2015.

[46] M. N. Tehrani, M. Uysal, and H. Yanikomeroglu, "Device-to-device communication in 5G cellular networks: Challenges, solutions, and future directions," *IEEE Communications Magazine*, vol. 52, no. 5, pp. 86–92, May 2014.

[47] George H. Brown and O. M. Woodward Jr., "Circularly Polarized Omnidirectional Antenna," *RCA Review*, vol. 8, no. 2, pp. 259-269, June 1947.

[48] B. Li, S. Liao and Q. Xue, "Omnidirectional Circularly Polarized Antenna Combining Monopole and Loop Radiators," *IEEE Antennas and Wireless Propagation Letters*, vol. 12, pp. 607-610, 2013.

[49] X. Chen, W. Zhang, L. Han, X. Chen, R. Ma and G. Han, "Wideband Circularly Polarized Antenna Realizing Omnidirectional Radiation in the Wider Azimuth Planes," *IEEE Antennas and Wireless Propagation Letters*, vol. 16, pp. 2461-2464, 2017.

[50] W. Lin, R. W. Ziolkowski and T. C. Baum, "28 GHz Compact Omnidirectional Circularly Polarized Antenna for Device-to-Device Communications in the Future 5G Systems," *IEEE Transaction on Antennas and Propagation*, vol. 65, no. 12, pp. 6904-6914, Dec. 2017

[51] X. Hu, S. Yan, J. Zhang, V. Volski and G. A. E. Vandenbosch, "Omni-Directional Circularly Polarized Button Antenna for 5 GHz WBAN Applications," *IEEE Transaction on Antennas and Propagation*, vol. 69, no. 8, pp. 5054-5059, Aug. 2021.

[52] Y. Shi and J. Liu, "Wideband and Low-Profile Omnidirectional Circularly Polarized Antenna With Slits and Shorting-Vias," *IEEE Antennas and Wireless Propagation Letters*, vol. 15, pp. 686-689, 2016.

[53] Y. Liu, X. Li, L. Yang and Y. Liu, "A Dual-Polarized Dual-Band Antenna With Omni-Directional Radiation Patterns," *IEEE Transaction on Antennas and Propagation*, vol. 65, no. 8, pp. 4259-4262, Aug. 2017.

[54] C. Guo, R. Yang and W. Zhang, "Compact Omnidirectional Circularly Polarized Antenna Loaded With Complementary V-Shaped Slits," *IEEE Antennas and Wireless Propagation Letters*, vol. 17, no. 9, pp. 1593-1597, Sept. 2018.

[55] D. Wu, X. Chen, L. Yang, G. Fu and X. Shi, "Compact and Low-Profile Omnidirectional Circularly Polarized Antenna With Four Coupling Arcs for UAV Applications," *IEEE Antennas and Wireless Propagation Letters*, vol. 16, pp. 2919-2922, 2017.

[56] Y. M. Pan and K. W. Leung, "Wideband Omnidirectional Circularly Polarized Dielectric Resonator Antenna With Parasitic Strips," *IEEE Transaction on Antennas and Propagation*, vol. 60, no. 6, pp. 2992-2997, June 2012.

[57] M. Khalily, M. R. Kamarudin, M. Mokayef and M. H. Jamaluddin, "Omnidirectional Circularly Polarized Dielectric Resonator Antenna for 5.2-GHz WLAN Applications," *IEEE Antennas and Wireless Propagation Letters*, vol. 13, pp. 443-446, 2014.

[58] J. Shi, X. Wu, X. Qing and Z. N. Chen, "An Omnidirectional Circularly Polarized Antenna Array," *IEEE Transaction on Antennas and Propagation*, vol. 64, no. 2, pp. 574-581, Feb. 2016.

[59] W. Lin and R. W. Ziolkowski, "Compact, High Directivity, Omnidirectional Circularly Polarized Antenna Array," *IEEE Transaction on Antennas and Propagation*, vol. 67, no. 7, pp. 4537-4547, July 2019.

List of Publications

I Journal Papers

[A1] S. Wu, J. Xu and Q. Chen, “A non-uniform collinear dipole array for sub-6 band,” *IEICE Communication Express*, Vol.X12-B, No.8, pp.-, Aug. 2023. DOI: https://doi.org/10.1587/comex. 2023TCL0018

[A2] S. Wu, J. Xu and Q. Chen, “High Gain Omnidirectional Horizontally Polarized Dipole Array for Sub-6 Base Station,” *IEEE Antennas and Wireless Propagation Letters*, doi: 10.1109/ LAWP.2023.3257385.

[A3] S. Wu, J. Xu and Q. Chen, “Omnidirectional Property and Gain Improvement of Circularly Polarized Collinear Antenna Arrayd,” *Microwave and Optical Technology Letters*. (major revision)

[A4] S. Wu, H. Sato and Q. Chen, “A composite antenna with high-gain at dual-band,” *IEICE Communication Express*, Vol.X12-B, No.8, pp.-,Aug. 2023. DOI: https://doi.org/10.1587/comex. 2023TCL0019

II Conference Papers with Peer Review

[B1] S. Wu, L. Wang, T. Kou and Q. Chen,“Collinear Super Turnstile Antennas for 5G Sub-6 Base Station,”*2020 International Symposium on Antennas and Propagation (ISAP)*, Osaka, Japan, 2021, pp. 763-764, doi: 10.23919/ISAP47053.2021.9391434.

III Conference Papers without Peer Review

[C1] S. Wu, J. Xu and Q. Chen,“Omnidirectional Property Enhancement of Circularly Polarized Collinear Antenna Array,”*IEICE Society Conference*, B-1-54, Sept. 2022.

[C2] S. Wu, L. Wang, T. Kou and Q. Chen,“Non-uniform Collinear Turnstile Antennas,”*2021 Tohoku-Section Joint Convention of Institutes of Electrical and Information Engineers*, Hachinohe, Japan, 4H01, Aug. 2021.

[C3] S. Wu, L. Wang, T. Kou and Q. Chen,“Dual-polarized Omni Antenna for Sub6 Base Station,”*IEICE Society Conference*, B-1-93, Sept. 2020.

[C4] S.Wu, H.Li, Q.Chen,“High Gain Omnidirectional Circularly Polarized Collinear Antenna Array for 5G Sub-6 Band,”伝送工学研究会，2022 年 5 月.

[C5] S. Wu, Q. Chen,“Non-uniform Collinear Turnstile Antennas for 5G Sub-6 Base Station,”伝送工学研究会，2021 年 5 月.

List of Awards

[D1] IEEE Sendai WIE Awards “The Best Paper Prize”, 2021 Tohoku-Section Joint Convention of Institutes of Electrical and Information Engineers, Japan.